AD NUMBER

AD817821

LIMITATION CHANGES

TO:

Approved for public release; distribution is unlimited.

FROM:

Distribution authorized to U.S. Gov't. agencies and their contractors; Critical Technology; JUL 1967. Other requests shall be referred to National Aeronautics and Space Administration, Goddard Space Flight Center, Greenbelt, MD. This document contains export-controlled technical data.

AUTHORITY

AEDC ltr, 4 Apr 1973

AEDC-TR-67-127

AUG 15 1967

SEP 18 1968

Cy 2

EVALUATION OF TWO RADIO ASTRONOMY EXPLORER SPACECRAFT APOGEE KICK MOTORS TESTED IN THE SPIN MODE AT SIMULATED ALTITUDE CONDITIONS

D. W. White and J. E. Harris

ARO, Inc.

July 1967

ROCKET TEST FACILITY
ARNOLD ENGINEERING DEVELOPMENT CENTER
AIR FORCE SYSTEMS COMMAND
ARNOLD AIR FORCE STATION, TENNESSEE

NOTICES

When U. S. Government drawings specifications, or other data are used for any purpose other than a definitely related Government procurement operation, the Government thereby incurs no responsibility nor any obligation whatsoever, and the fact that the Government may have formulated, furnished, or in any way supplied the said drawings, specifications, or other data, is not to be regarded by implication or otherwise, or in any manner licensing the holder or any other person or corporation, or conveying any rights or permission to manufacture, use, or sell any patented invention that may in any way be related thereto.

Qualified users may obtain copies of this report from the Defense Documentation Center.

References to named commercial products in this report are not to be considered in any sense as an endorsement of the product by the United States Air Force or the Government.

EVALUATION OF TWO RADIO ASTRONOMY EXPLORER SPACECRAFT APOGEE KICK MOTORS TESTED IN THE SPIN MODE AT SIMULATED ALTITUDE CONDITIONS

D. W. White and J. E. Harris
ARO, Inc.

AF AEDC
Arnold AFS Tenn

FOREWORD

The test program reported herein was conducted under the sponsorship of the National Aeronautics and Space Administration (NASA), Goddard Space Flight Center (GSFC), for the Thiokol Chemical Corporation (TCC), Elkton Division, under Program Area 921E, Project 9033.

The results of the test were obtained by ARO, Inc. (a subsidiary of Sverdrup & Parcel and Associates, Inc.), contract operator of the Arnold Engineering Development Center (AEDC), Air Force Systems Command (AFSC), Arnold Air Force Station, Tennessee, under Contract AF 40(600)-1200. The test was conducted in Propulsion Engine Test Cell (T-3) of the Rocket Test Facility (RTF) from March 24 to 31, 1967, under ARO Project Number RC1710, and the manuscript was submitted for publication on May 27, 1967.

Information in this report is embargoed under the Department of State International Traffic in Arms Regulations. This report may be released to foreign governments by departments or agencies of the U.S. Government subject to approval of the National Aeronautics and Space Administration (NASA), Goddard Space Flight Center.

This technical report has been reviewed and is approved.

Joseph R. Henry
Lt Col, USAF
AF Representative, RTF
Directorate of Test

Leonard T. Glaser
Colonel, USAF
Director of Test

ABSTRACT

Two Thiokol Chemical Corporation TE-M-479 solid-propellant apogee rocket motors each installed in a Radio Astronomy Explorer (RAE) spacecraft shell were fired at average pressure altitudes in excess of 118,000 ft while spinning at 75 rpm. The primary objectives of the test were to: evaluate the ignition characteristics of the motor when ignited with one Pyrogen igniter, determine motor vacuum ballistic performance when pre-conditioned at 40 and 90°F, evaluate motor tailoff characteristics, and evaluate motor structural integrity and determine motor temperature-time history during and after motor operation. Secondary objectives were to measure motor thrust misalignment and thermal inputs into the RAE spacecraft resulting from motor operation. Both motors ignited satisfactorily. Vacuum specific impulse values for the 40 and the 90°F motors were 289.97 and 290.63 lb_f-sec/lb_m, respectively, based on the manufacturer's stated propellant weight.

CONTENTS

APPENDIXES

I. ILLUSTRATIONS

Figure

NOMENCLATURE

P_{max}	Maximum chamber pressure, the highest chamber pressure developed during normal operation, excluding ignition transients, psia
t_a	Action time, time interval between 10 percent of maximum chamber pressure during ignition and 10 percent of maximum chamber pressure during tailoff, sec
t_{f_b}	Full duration burn time, interval from time of increase in thrust during ignition to time that thrust has decreased to zero during tailoff, sec
t_d	Ignition delay time, time interval from zero time until chamber pressure has risen to 10 percent of maximum chamber pressure, sec
t_ℓ	Ignition lag time, interval from zero time to time of increase in chamber pressure, sec
t_o	Zero time, time at which firing voltage is applied to the ignition circuit, sec

SECTION I
INTRODUCTION

The Thiokol Chemical Corporation (TCC) TE-M-479 solid-propellant rocket motor is to be used as the Apogee Kick Motor for the Radio Astronomy Explorer (RAE) spacecraft (Fig. 1, Appendix I). The scientific objective of the RAE mission is to measure the frequency, intensity, and source direction of radio signals from solar, galactic, and extra-galactic sources. The spacecraft will accomplish the first mapping of our galaxy at frequencies below ionospheric cutoff. The spacecraft antennas will consist of two V antennas formed by deploying four booms, 0.5 in. in diameter and 750 ft in length. A third antenna will consist of a dipole deployed normal to the Z (longitudinal) axis of the spacecraft (Ref. 1).

Accomplishment of the RAE project objectives requires placement of a gravity-gradient captured spacecraft in a 3728-mile circular orbit with a minimum operational lifetime of one year. To accomplish this, the spacecraft must be placed in a transfer orbit of 342-mile perigee, 3728-mile apogee and be spin stabilized at 80 rpm by the launch vehicle. The apogee kick motor must be fired when properly oriented at apogee to place the spacecraft in a 3728-mile circular orbit. After burnout, the apogee motor must be ejected, and the spacecraft must be despun to 10 rpm or less by a yo-yo despin device. The spacecraft will ultimately be despun to 0 rpm and magnetically positioned for ultimate gravity gradient capture (Ref. 1).

The primary objectives of the test reported herein were to: evaluate the altitude ignition characteristics of the TE-M-479 rocket motor when ignited with one Pyrogen igniter, determine the altitude ballistic performance of the TE-M-479 rocket motor when spinning at 75 rpm after prefire temperature conditioning at 40 ± 5°F (one motor) and 90 ± 5°F (one motor), evaluate motor tailoff performance characteristics, and evaluate the structural integrity of the TE-M-479 rocket motor and determine motor temperature-time history during and after motor operation. Secondary objectives were to measure motor thrust misalignment and thermal inputs to the RAE spacecraft resulting from rocket motor operation.

Motor altitude, ballistic performance, and structural integrity are discussed along with motor thrust misalignment.

SECTION II
APPARATUS

2.1 TEST ARTICLE

The TCC TE-M-479 solid-propellant rocket motor (Fig. 2) is a full-scale, flightweight motor having the following nominal dimensions and burning characteristics at 90°F:

Length, in.	27
Diameter, in.	17.5
Loaded Weight, lb_m	175
Propellant Weight, lb_m	153
Maximum Thrust, lb_f	2865
Maximum Chamber Pressure, psia	910
Burn Time, sec	20
Throat Area, $in.^2$	1.48
Nozzle Area Ratio, A/A*	60

The cylindrical motor case is constructed of 0.040-in. titanium. The case is lined internally with TCC TL-H-304 liner and insulated with asbestos-filled Buna-N rubber. A pressure relief boot assembly is contained in the forward end of the motor case (Fig. 2). A flange located on the aft dome provides for attachment to the RAE spacecraft.

The contoured nozzle assembly contains a Graph-I-Tite G-90 carbon throat insert and an expansion cone constructed of Vitreous Silica Phenolic. The nozzle assembly has a nominal 60:1 area ratio and a 15-deg half-angle at the exit plane. A Styrofoam® closure was bonded in the nozzle expansion cone. The closure was punctured prior to test so that the rocket motor chamber pressure was equal to test cell pressure at motor ignition.

The TE-M-479 rocket motor contains a propellant grain formulation designated TP-H-3062 (ICC Class B), cast in an eight-point star configuration. The isentropic exponent of the propellant exhaust gases is 1.18 (assuming frozen equilibrium).

Ignition was accomplished by a TE-P-386-7 Pyrogen igniter (Fig. 3) which contained 20, size 2A Boron pellets used to initiate the primary

Poly-sulfide igniter grain. Nominal ignition current was 4 amp and was maintained for approximately 0.3 sec. The motor contained two pyrogen igniters; however, only one igniter was used in these tests.

The motors were mounted and fired in a RAE spacecraft shell (flightweight, without sensors) to determine thermal effects of the apogee motor firing on the flightweight spacecraft instrumentation payload.

2.2 INSTALLATION

The motor-spacecraft assembly was cantilever mounted from the spindle face of a spin fixture assembly in Propulsion Engine Test Cell (T-3) (Ref. 2). The spin assembly was mounted on a thrust cradle, which was supported from the cradle support stand by three vertical and two horizontal double-flexure columns (Fig. 4). The spin fixture assembly consists of a 10-hp squirrel-cage-type drive motor, a forward thrust bearing assembly, a 46-in.-long spindle having a 36-in.-diam aft spindle face, and an aft bearing assembly. The spin fixture was rotated counterclockwise, looking upstream. Electrical leads to and from the igniters, pressure transducers, and thermocouples on the rotating motor were provided through a 170-channel, slip-ring assembly mounted between the forward and aft bearing assemblies on the spindle. Axial thrust was transmitted through the spindle-thrust bearing assembly to two load cells mounted just forward of the thrust bearing.

Pre-ignition pressure altitude conditions were maintained in the test cell by a steam ejector operating in series with the RTF exhaust gas compressors. During a motor firing, the motor exhaust gases were used as the driving gas for the 36-in.-diam, ejector-diffuser system to maintain test cell pressure at an acceptable level.

2.3 INSTRUMENTATION

Instrumentation was provided to measure axial thrust, motor chamber pressure, test cell pressure, lateral force, motor case and nozzle temperatures, rotational speed, and spacecraft temperatures. Table I (Appendix II) presents instrument ranges, recording methods, and system accuracies for all reported parameters.

The axial thrust measuring system consisted of two double-bridge, strain-gage-type load cells mounted in the axial double-flexure column forward of the thrust bearing on the spacecraft centerline. The lateral

force measuring system consisted of double-bridge, strain-gage-type load cells installed forward and aft between the flexure-mounted cradle and the cradle support stand normal to the rocket motor axial centerline and in the horizontal plane passing through the motor axial centerline (Fig. 4c).

Unbonded strain-gage-type transducers were used to measure test cell pressure and low-range (0- to 1-psia) chamber pressure. Bonded strain-gage-type transducers with ranges of 0 to 50 and 0 to 1000 psi were used to measure motor chamber pressures. Iron-constantan (IC) thermocouples were bonded to the motor case and nozzle (Fig. 5) to measure outer surface temperatures during and after motor burn time. Copper-constantan (CC) thermocouples were bonded to the spacecraft and motor attachment hardware (Fig. 6) to measure increases in temperatures resulting from motor operation. Rotational speed of the motor-spacecraft assembly was determined from the output of a magnetic pickup.

The output signal of each measuring device was recorded on independent instrumentation channels. Primary data were obtained from four axial thrust channels (three channels for motor S/N 7), three test cell pressure channels, and four motor chamber pressure channels. These primary data were recorded as follows: Each instrument output signal was indicated in totalized digital form on a visual readout of a millivolt-to-frequency converter. A magnetic tape system, recording in frequency form, stored the signal from the converter for reduction at a later time by an electronic digital computer. The computer provided a tabulation of average absolute values for each 0.10-sec time increment and total integrals over the cumulative time increments.

The output signal from the magnetic rotational speed pickup was recorded in the following manner: A frequency-to-analog converter was triggered by the pulse output from the magnetic pickup and in turn supplied a square wave of constant amplitude to the electronic counter and oscillograph recorder. The scan sequence of the electronic counter was adjusted so that it displayed directly the motor spin rate in revolutions per minute.

The millivolt outputs of the thermocouples were recorded on magnetic tape from a multi-input, analog-to-digital converter at a sampling rate for each thermocouple of 75 samples per second. The millivolt outputs of the lateral force load cells were recorded on FM analog magnetic tape and played back through a filter system to an oscillograph and a digital magnetic tape recorder at a later time.

A recording oscillograph was used to provide an independent backup of all operating instrumentation channels except the temperature and side

force systems. Selected channels of thrust and pressures were recorded on null-balance, potentiometer-type strip charts for analysis immediately after a motor firing. Visual observation of each firing was provided by a closed-circuit television monitor. High-speed, motion-picture cameras provided a permanent visual record of each firing.

2.4 CALIBRATION

The thrust calibrator weights, axial and lateral force load cells, and pressure transducers were laboratory calibrated prior to usage in this program. After installation of the measuring devices in the test cell, all systems were calibrated at ambient conditions and again at simulated altitude conditions just before a motor firing.

The pressure systems were calibrated by an electrical, four-step calibration, using resistances in the transducer circuits to simulate selected pressure levels. The axial thrust instrumentation systems were calibrated by applying to the thrust cradle known forces which were produced by deadweights acting through a bell crank. The calibrator is hydraulically actuated and remotely operated from the control room. The side force instrumentation systems were calibrated by an electrical, four-step calibration, using resistances in the circuits to simulate selected force levels. Thermocouple systems were calibrated by using known millivolt levels to simulate selected thermocouple outputs.

After each motor firing, with the test cell still at simulated altitude pressure, the systems were again recalibrated to determine if any shift had occurred.

SECTION III
PROCEDURE

The two TCC TE-M-479 rocket motors (S/N's 7 and 10) and the RAE spacecraft shell arrived at AEDC on March 6 and 7, respectively. The motors were visually inspected for possible shipping damage and radiographically inspected for grain cracks, voids, or separations and found to meet criteria provided by the manufacturer. During storage in an area temperature conditioned at 70 ± 5°F, the motors and spacecraft were checked to ensure correct fit of mating hardware, and the electrical resistances of the igniters were measured. The pre-punctured nozzle closures were removed, the nozzle throat and exit diameters were obtained, the nozzle closures were reinstalled, and the motors were weighed. Thermocouples were bonded to the nozzle and motor case, and the entire motor assembly was weighed and photographed.

The spacecraft arrived with thermocouples installed and personnel from NASA-GSFC performed checkouts of these systems. A motor was installed in the spacecraft, and radial dimensions of selected surfaces as a function of angular position relative to the spin axis of the spacecraft and rocket motor were then determined by NASA-GSFC personnel to facilitate alignment of the motor-spacecraft assembly in the test cell.

After installation of the motor-spacecraft assembly in the test cell, the spacecraft centerline was axially aligned with the spin axis by rotating the motor spacecraft assembly and measuring the deflection of the spacecraft surfaces with a dial indicator. The eccentricity between the spacecraft centerline and spin axis was 0.001 in. for motor S/N 7 and 0.002 in. for motor S/N 10. Instrumentation connections were made, and the motor-spacecraft assembly was balanced at a rotational speed of 75 rpm. Temperature conditioning of the motor-spacecraft assembly (40°F, motor S/N 7 and 90°F, motor S/N 10) was begun and continued for a period in excess of 22 hr. The two Pyrogen igniters were installed, the motor was leak checked, and a continuity check of all electrical systems was performed. Pre-fire ambient calibrations were completed, the test cell pressure was reduced to simulate the desired altitude, and spinning of the unit was started. After spinning had stabilized at 75 rpm, a complete set of altitude calibrations was taken.

The final operation prior to firing a motor was to adjust the firing circuit resistance to provide the desired current (4 amp) to the igniter squib (the motor contained two igniters; however, only one was used to ignite a motor). The entire instrumentation measuring-recording complex was activated, and the motor was fired while spinning (under power) at 75 rpm.

Spinning of the motor was continued for approximately 45 min after burnout, during which time motor and spacecraft temperatures were recorded and post-fire calibrations were accomplished. The unit was decelerated slowly until rotation had stopped, and another set of calibrations was taken. The test cell pressure was then returned to ambient conditions, and the motor-spacecraft assembly was inspected, photographed, and removed to the storage area. Post-fire inspections at the storage area consisted of measuring the throat and exit diameters of the nozzle, weighing the motor, and photographically recording the post-fire condition of the motor.

SECTION IV
RESULTS AND DISCUSSION

Two Thiokol Chemical Corporation TE-M-479 solid-propellant rocket motors (S/N's 7 and 10) were fired in Propulsion Engine Test Cell (T-3) while mounted in an RAE spacecraft shell (flightweight, without sensors). The motors were pre-fire temperature conditioned at 40 ± 5°F (motor S/N 7) and 90 ± 5°F (motor S/N 10) for periods in excess of 22 hr and fired at average pressure altitudes in excess of 118,000 ft with the motor-spacecraft assembly spinning about the spacecraft longitudinal axis at 75 rpm. The primary objectives of the test program were to: evaluate the ignition characteristics of the motors when ignited with one Pyrogen igniter, determine motor altitude ballistic performance at 40 and 90°F, evaluate motor tailoff characteristics, and evaluate motor structural integrity and determine motor temperature-time history during and after motor operation. Secondary objectives were to measure motor thrust misalignment and thermal inputs into the RAE spacecraft resulting from motor operation. The resulting data are presented in both tabular and graphical form. Motor performance data based on action time (t_a) and full-duration burn time (t_{f_b}) are summarized in Table III. The average measured total impulse values were corrected to vacuum by adding the product of the cell pressure integral and the average of the pre- and post-fire nozzle exit areas. The average vacuum correction was approximately 0.30 and 0.23 percent of the average measured total impulse for motors S/N 7 and 10, respectively. Specific impulse values are presented using both the manufacturer's stated propellant weight and the motor expended mass determined from AEDC pre- and post-fire motor weights. When multiple channels of equal accuracy instrumentation were used to obtain values of a single parameter, the average value was used to calculate the data presented.

4.1 ALTITUDE IGNITION CHARACTERISTICS

The motors were ignited at pressure altitudes of 124,000 ft (S/N 7) and 127,000 ft (S/N 10) with the pre-punctured nozzle closure bonded in place. An analog trace of a typical ignition event is shown in Fig. 7. Ignition lag times (t_ℓ) were 0.010 and 0.011 sec for motor S/N 7 and motor S/N 10, respectively. Ignition delay times (t_d) were 0.069 sec (S/N 7) and 0.063 sec (S/N 10). The effects of the spare Pyrogen igniting are evident in Fig. 7.

4.2 ALTITUDE BALLISTIC PERFORMANCE

Variations of thrust, chamber pressure, and cell pressure during each firing are shown in Fig. 8. Performance characteristics for both motors are tabulated below:

Motor S/N	7	10
Pre-Fire Motor Temperature, °F	40	90
Action Time (t_a), sec	19.5	18.2
Full-Duration Burn Time (t_{f_b}), sec	21.4	20.2
Vacuum Total Impulse, Based on t_{f_b}, lb_f-sec	44,406	44,583
Vacuum Specific Impulse, Based on t_{f_b} and the Manufacturer's Stated Propellant Weight, lb_f-sec/lb_m	289.97	290.63
Vacuum Specific Impulse, Based on t_{f_b} and Expended Mass, lb_f-sec/lb_m	285.97	286.65
Average Vacuum Thrust Coefficients, Based on t_a and the Average Pre- and Post-Fire Throat Area	1.846	1.854

The motor conditioned at 90°F had a vacuum specific impulse value of approximately 0.7 lb_f-sec/lb_m greater than the motor conditioned at 40°F.

A comparison of low-range chamber pressure and test cell pressure during both motor firings is presented in Fig. 9. An increase in low-range chamber pressure was evident at approximately 54 sec after ignition of motor S/N 7. The increase in chamber pressure reached a maximum of 0.3 psia approximately 68 sec after ignition and returned to the cell pressure level at approximately 108 sec after ignition. A similar increase in low-range chamber pressure was evident at approximately 40 sec after ignition of motor S/N 10. The increase in pressure reached a maximum of 0.16 psia approximately 56 sec after ignition and returned to the cell pressure level at approximately 108 sec after motor ignition. These increases in chamber pressure are believed to have resulted from smoldering insulator and/or liner. The impulse accumulated during these respective periods was negligible.

4.3 STRUCTURAL INTEGRITY

External post-fire examination of the motor cases did not reveal any distortion or evidence of thermal damage (Fig. 10a). Internal post-fire examination of the motor chambers revealed that the insulation had experienced a degree of charring (Fig. 10b); however, no degradation of the motor chamber was evident.

Photographs showing typical pre- and post-fire conditions of a nozzle exit cone are presented in Fig. 11. The nozzle throat inserts fell into the motor chamber following motor burnout. Photographs showing the post-fire condition of the nozzle throat inserts are presented in Fig. 12. Nozzle throat measurements indicated that erosion had caused an area increase of 22.7 and 24 percent from the pre-fire areas of motors S/N's 7 and 10, respectively.

Motor case and nozzle temperatures are presented in Figs. 13 through 16. Maximum case temperature measured on motor S/N 7 was 691°F, occurring approximately 263 sec after motor ignition on thermocouple T4, located over a propellant grain valley (Fig. 5). The maximum case temperature for motor S/N 10 was 654°F, occurring approximately 290 sec after motor ignition on thermocouple T4, located over a propellant grain star (Fig. 5). Both thermocouples were located 3.8 in. forward of the motor equator on the forward hemisphere.

Post-fire examination of the spacecraft after firing of motor S/N 7 revealed that the fiber glass element of the motor ejection piston assembly had been exposed to a high temperature source in a localized area (Fig. 17). The outer layer of fiber glass had separated and was touching the motor case. Prior to the second firing (motor S/N 10), the separated layer of fiber glass was removed. Post-fire examination of the spacecraft after firing of motor S/N 10 did not reveal any further thermal damage to the fiber glass element. A thermocouple was located on the reverse side of the fiber glass element (Fig. 6), and maximum temperatures of 655 (S/N 7) and 458°F (S/N 10) were recorded. These maximums occurred at 296 (S/N 7) and 480 (S/N 10) sec after ignition. Maximum temperature levels for the other 45 spacecraft thermocouples ranged from 48 to 160°F and 98 to 206°F for motors S/N's 7 and 10, respectively.

4.4 EXTRANEOUS THRUST VECTOR MEASUREMENTS

A secondary objective for this test was the measurement of motor thrust misalignment. This objective was accomplished by measuring the extraneous (lateral) component of the axial thrust. The recorded lateral thrust data were treated to eliminate or correct for installation and/or electronic effects as described in Appendix III. The resultant data are presented in Figs. 18 and 19.

The extraneous thrust values recorded for both motor firings exhibited similar characteristics during the time that thrust was increasing from zero to its steady-state magnitude (approximately 2500 lb_f). Both motors exhibited peaks in extraneous thrust vector magnitudes during

the time interval from ignition to approximately 2 sec after ignition. These values are considered questionable because of undefinable dynamic characteristics of the system under impact loading. It should be noted that these effects occur only during the buildup and tailoff portions of the thrust-time history of motor operation. Because of the uncertainties inherent in the extraneous thrust vector data recorded during the ignition transient, they will not be considered in the following discusssion.

Maximum lateral thrust magnitudes during the near steady-state portion of motor operation of 1.95 lb_f (9.62 sec after ignition) and 2.20 lb_f (11.88 sec after ignition) were recorded for motors S/N's 7 and 10, respectively. The corresponding angular positions (measured clockwise, looking upstream, from the motor chamber pressure port) were 175 deg (S/N 7) and 256 deg (S/N 10).

The resultant lateral thrust magnitudes were not corrected for lateral force caused by misalignment of the spacecraft-motor configuration on the spin fixture. The angular misalignment of the motor thrust axis with respect to the spin axis was 0.0043 deg for motor S/N 7 and 0.0059 deg for motor S/N 10. These values of angular misalignment resulted in lateral thrust magnitudes of 0.21 lb_f (S/N 7) and 0.29 lb_f (S/N 10) at the maximum thrust level.

The inaccuracy of the force measuring system for this test is estimated to be ±0.27 lb_f (Appendix III). The total system inaccuracy, therefore, is the sum of the measuring inaccuracy and the thrust magnitude resulting from misalignment. The lateral thrust magnitudes, therefore, are accurate within ±0.48 lb_f for motor S/N 7 and ±0.56 lb_f for motor S/N 10.

SECTION V
SUMMARY OF RESULTS

Two Thiokol Chemical Corporation TE-M-479 solid-propellant rocket motors were fired at average pressure altitudes in excess of 118,000 ft while mounted in a Radio Astronomy Explorer (RAE) Spacecraft shell which was spinning at 75 rpm about the spacecraft axis. The motors were pre-fire temperature conditioned at 40 ± 5°F and 90 ± 5°F for periods in excess of 22 hr prior to firing. Results are summarized as follows:

1. The time interval from the time at which firing voltage was applied to the igniter circuit to the time of increase in chamber pressure was 0.010 sec for the motor temperature conditioned at 40°F and 0.011 sec for the motor temperature conditioned at 90°F.

2. The time interval between 10 percent of maximum chamber pressure during ignition and 10 percent of maximum chamber pressure during tailoff (t_a) was 19.5 sec for the 40°F motor and 18.2 sec for the 90°F motor.

3. The time interval from time of increase in thrust during ignition to the time that thrust has decreased to zero during tailoff (t_{f_b}) was 21.4 sec for the 40°F motor and 20.2 sec for the 90°F motor.

4. Vacuum total impulse, based on t_{f_b}, was 44,406 lb_f-sec for the 40°F motor and 44,583 lb_f-sec for the 90°F motor. Vacuum specific impulse based on t_{f_b} and the manufacturer's stated propellant weight was 289.97 lb_f-sec/lb_m for the 40° F motor and 290.63 lb_f-sec/lb_m for the 90°F motor.

5. The average thrust coefficients, based on t_a and the average pre- and post-fire throat areas, were 1.846 for the 40°F motor and 1.854 for the 90°F motor.

6. The nozzle throat areas increased 22.7 and 24 percent from the pre-fire areas for the 40 and 90°F motors, respectively. No evidence of motor case degredation was evident after a firing.

7. The maximum motor case temperatures were 691°F for the 40°F motor and 654°F for the 90°F motor. The times from ignition that these temperatures occurred were 263 sec for the 40°F motor and 290 sec for the 90°F motor.

8. Maximum extraneous thrust magnitudes occurring during the steady-state portion of the thrust curve of 1.95 lb_f (40°F motor) and 2.20 lb_f (90°F motor) were recorded. The angular positions of the thrust vectors at the time of maximum magnitude were approximately 175 and 256 deg from the motor chamber pressure port, measured clockwise looking upstream for the 40 and 90°F motors, respectively.

9. Each motor experienced low level pressure operation, after propellant burnout, for approximately 85 sec. These low level pressures are believed to have resulted from smoldering insulator and/or liner.

REFERENCES

1. "RAE Project Development Plan." NASA, Goddard Spaceflight Center, July 1966.

2. Test Facilities Handbook (6th Edition). "Rocket Test Facility, Vol. 2." Arnold Engineering Development Center, November 1966.

3. Nelius, M. A. and Harris, J. E. "Measurement at Nonaxial Forces Produced by Solid-Propellant Rocket Motors Using a Spin Technique." AEDC-TR-65-228 (AD474410), November 1965.

APPENDIXES

I. ILLUSTRATIONS
II. TABLES
III. CALIBRATION OF EXTRANEOUS THRUST VECTOR MEASURING SYSTEM TO DETERMINE SYSTEM ACCURACY

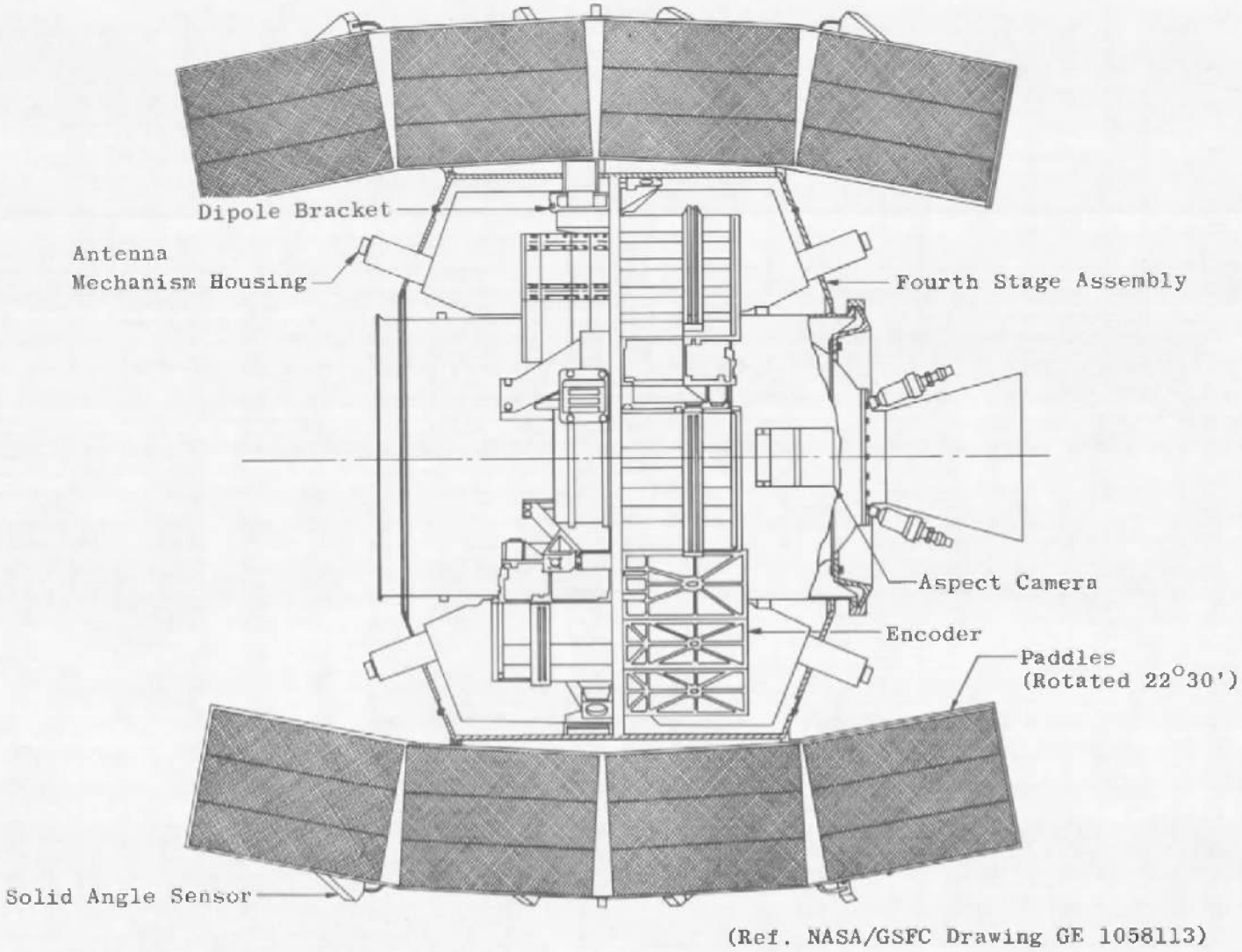

a. Schematic

Fig. 1 Radio Astronomy Explorer (RAE) Spacecraft

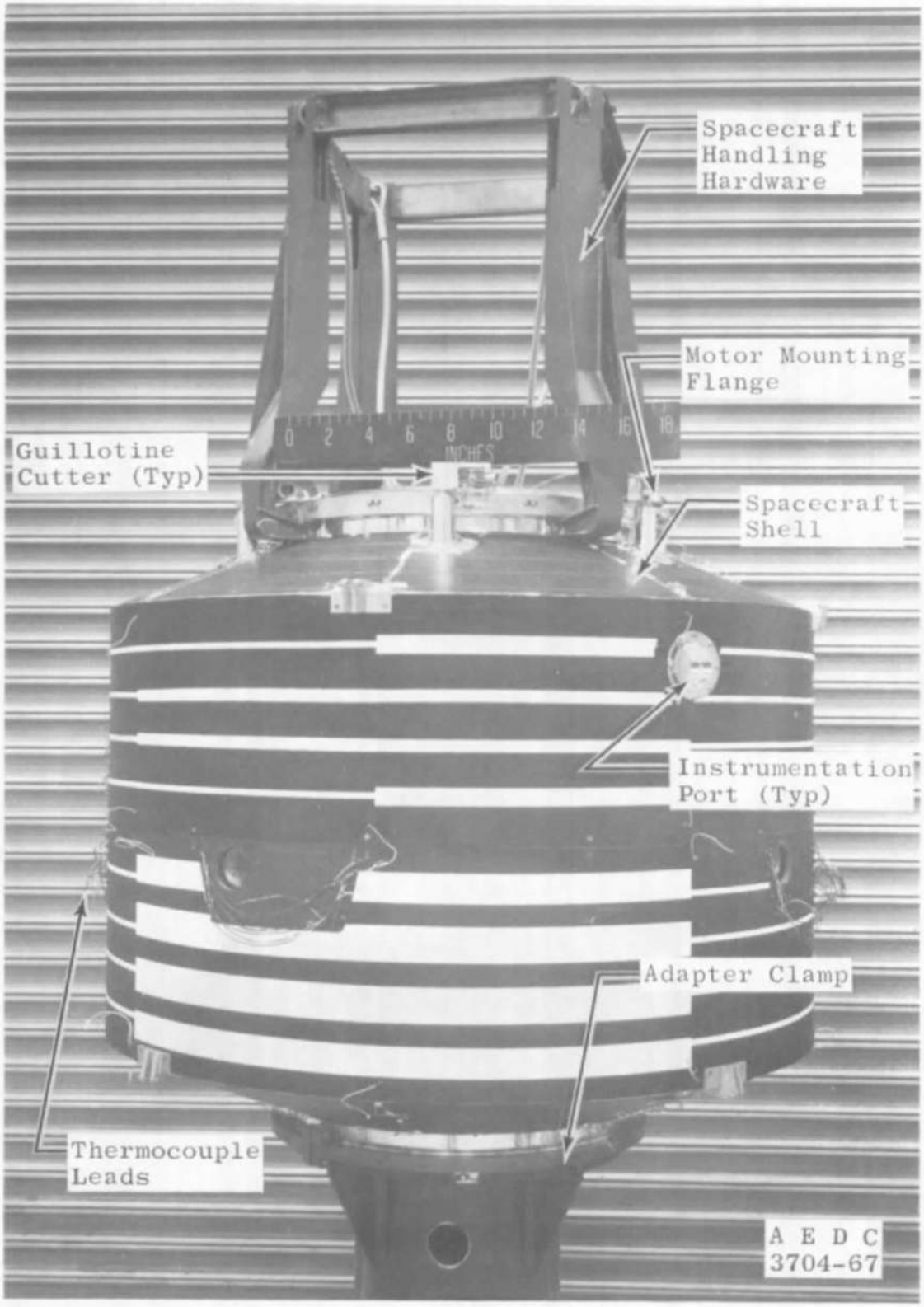

b. Photograph

Fig. 1 Concluded

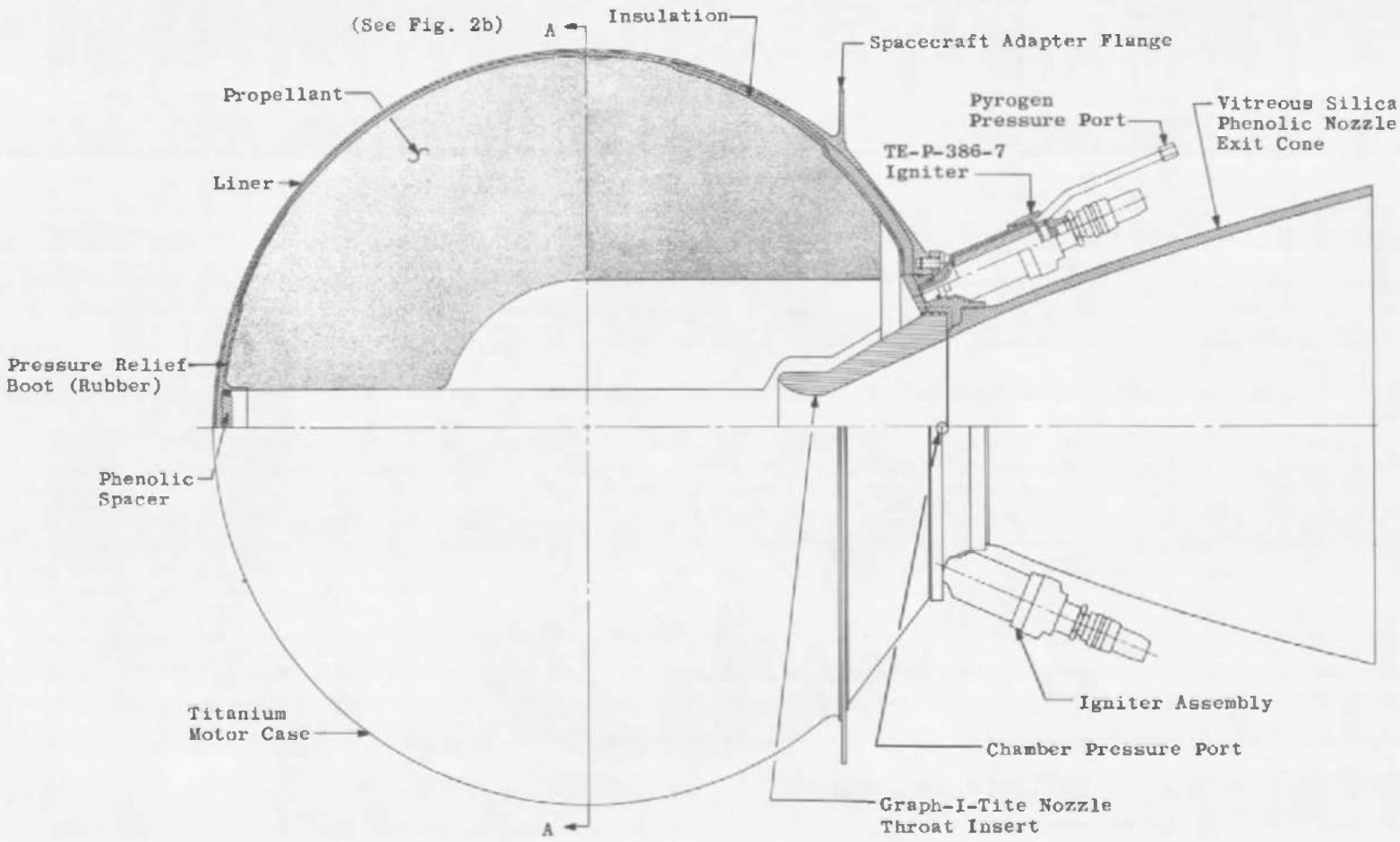

a. Motor Schematic

Fig. 2 TE-M-479 Rocket Motor

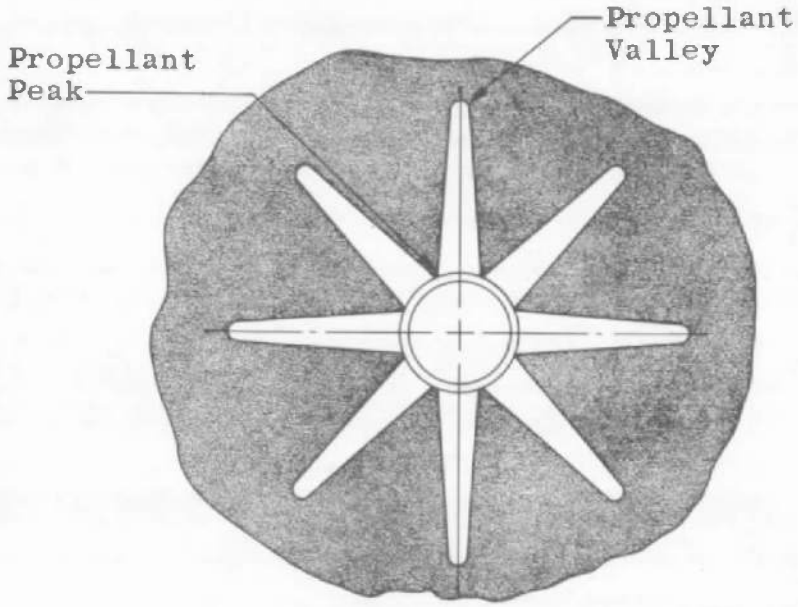

Section A-A

b. Propellant Schematic

Fig. 2 Continued

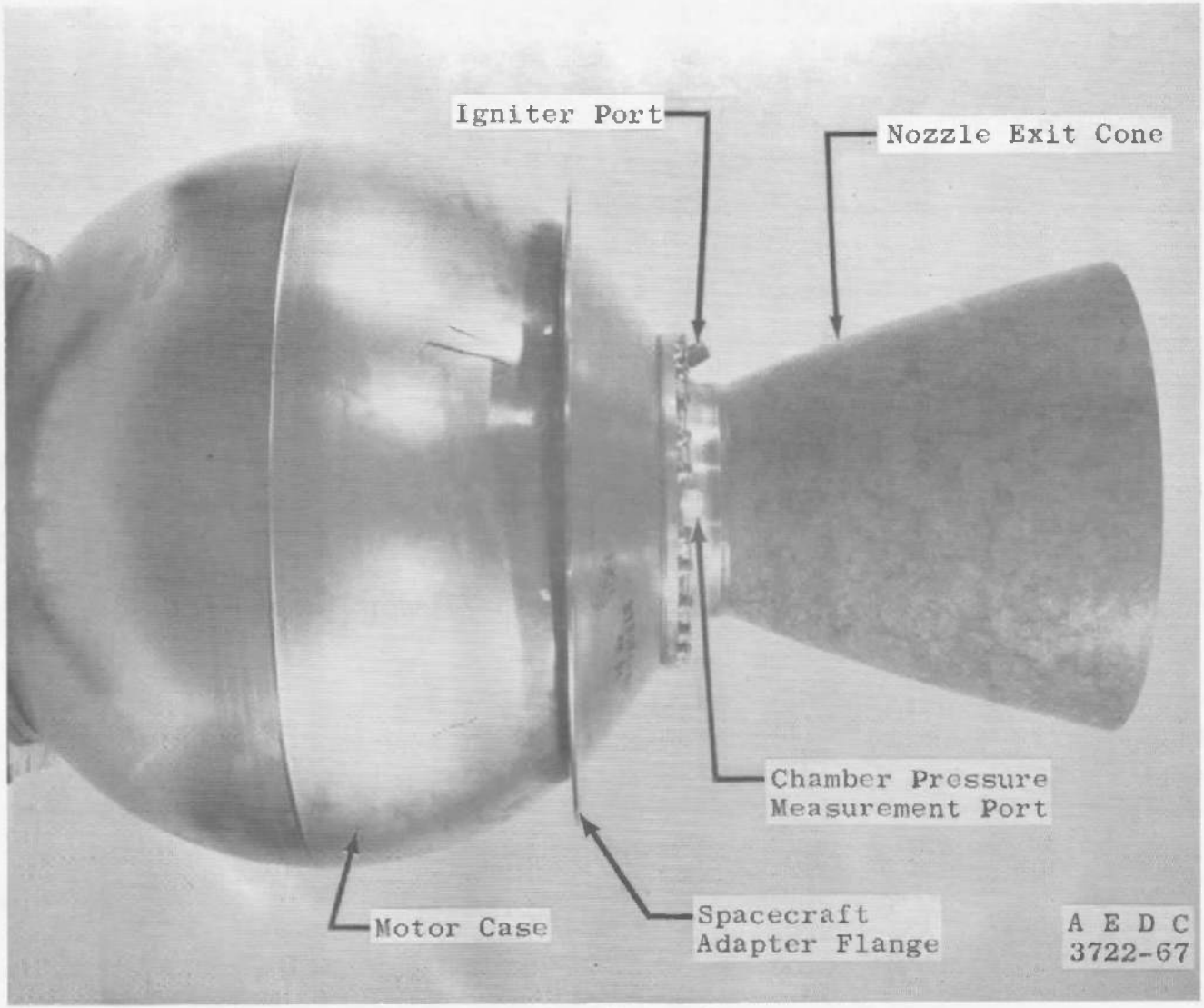

c. Motor Photograph

Fig. 2 Concluded

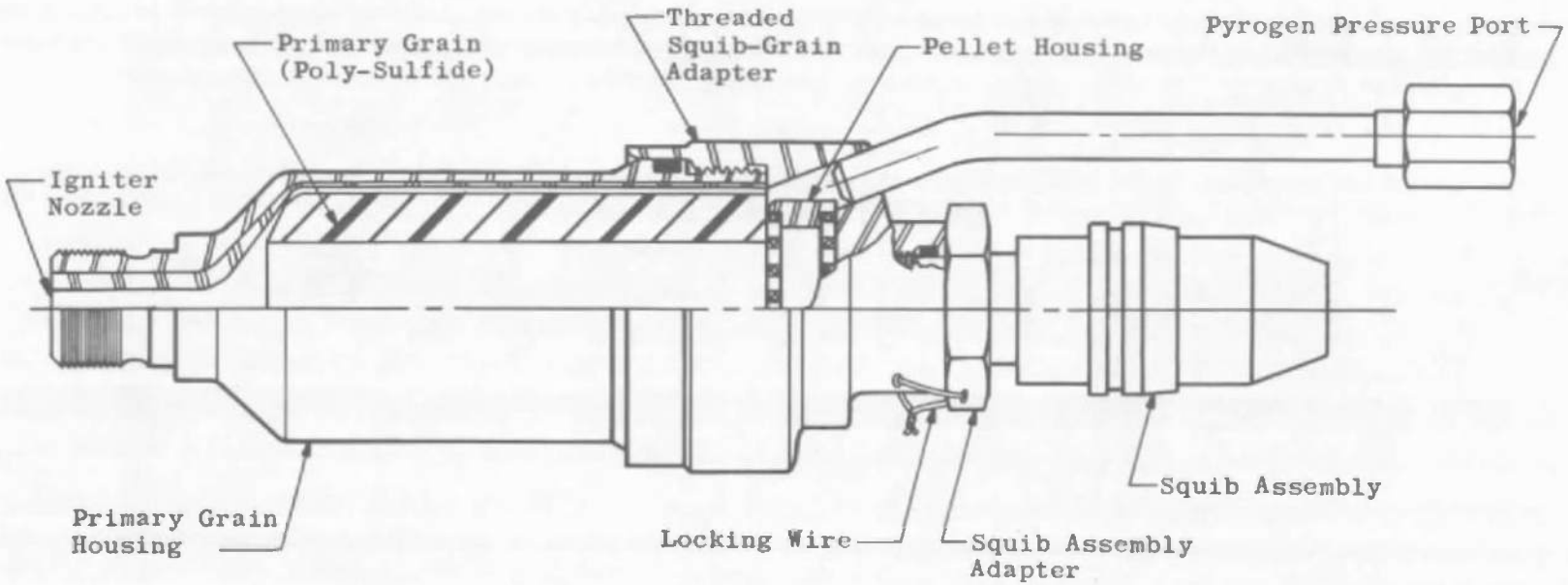

a. Schematic

Fig. 3 TE-P-386-7 Igniter

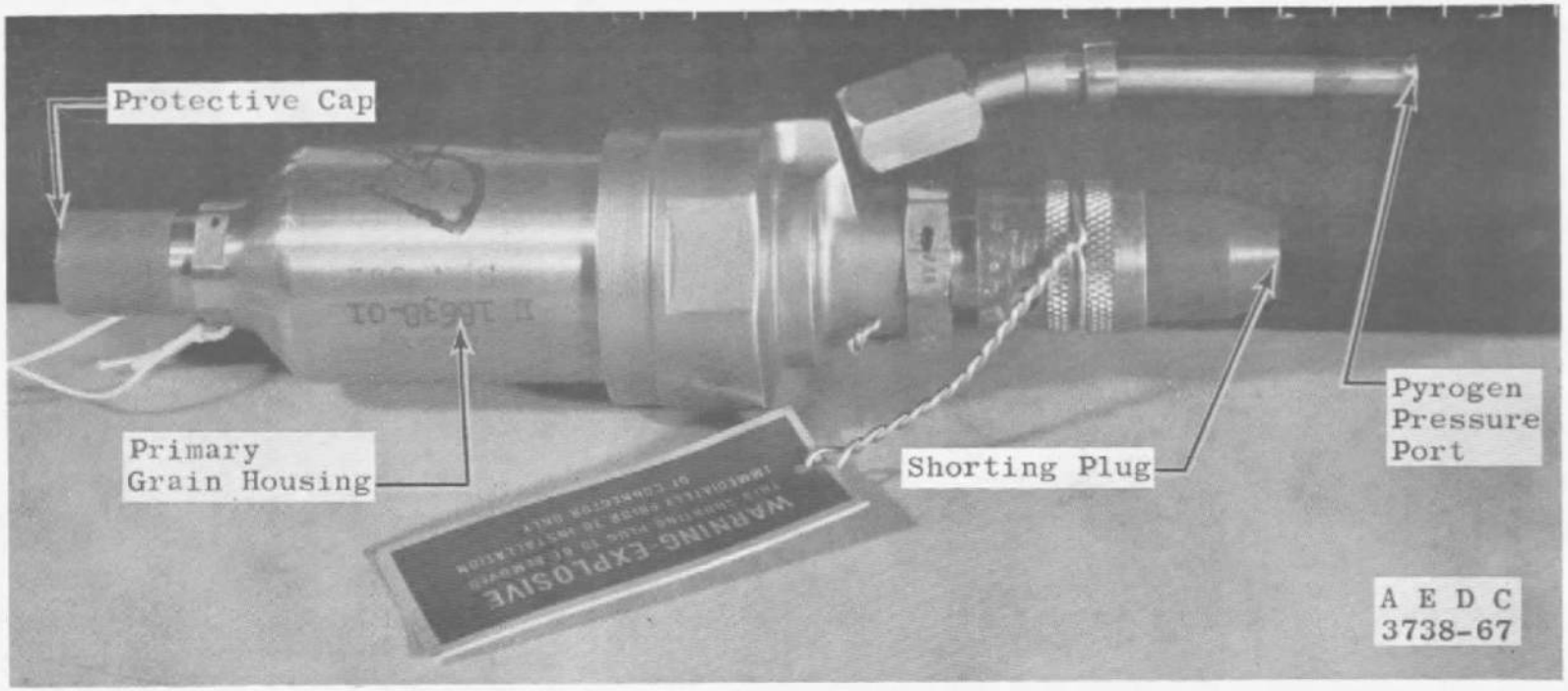

b. Photograph

Fig. 3 Concluded

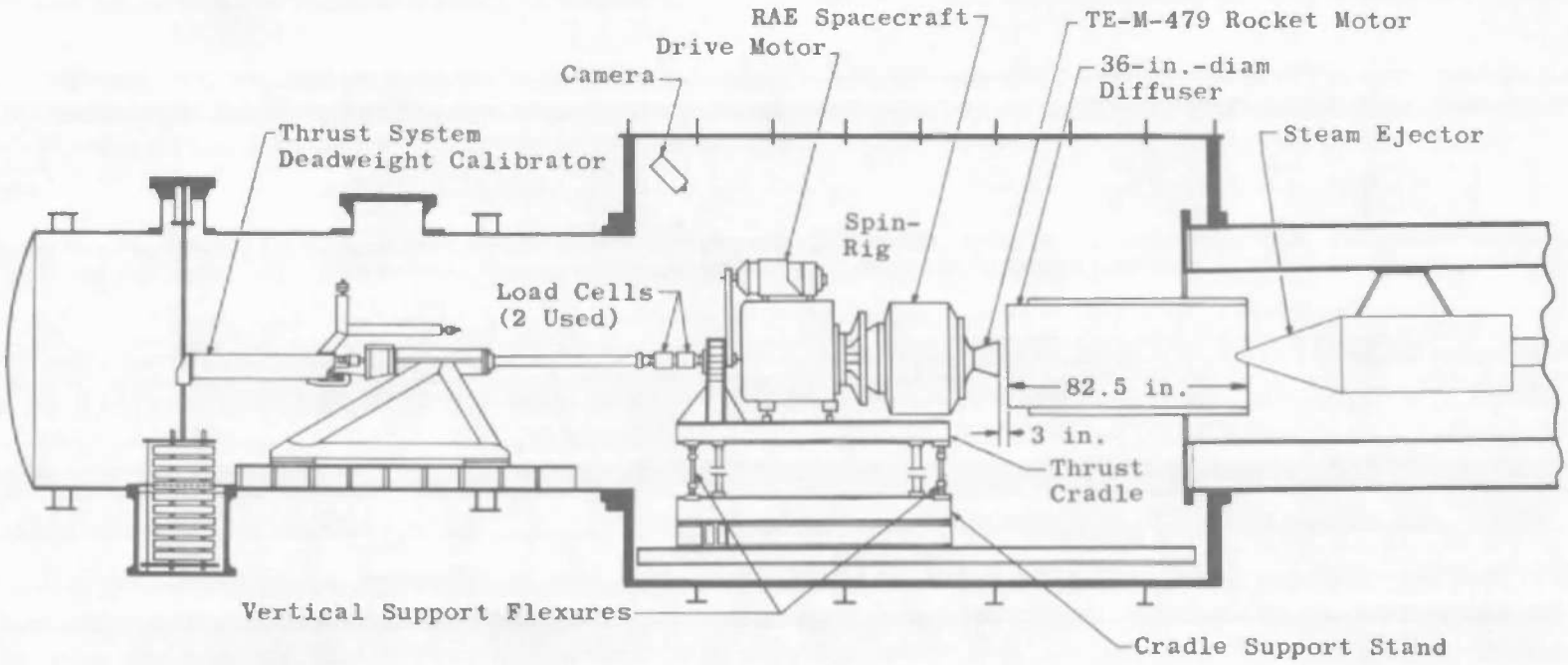

a. Schematic

Fig. 4 Installation of RAE Spacecraft Assembly in Propulsion Engine Test Cell (T-3)

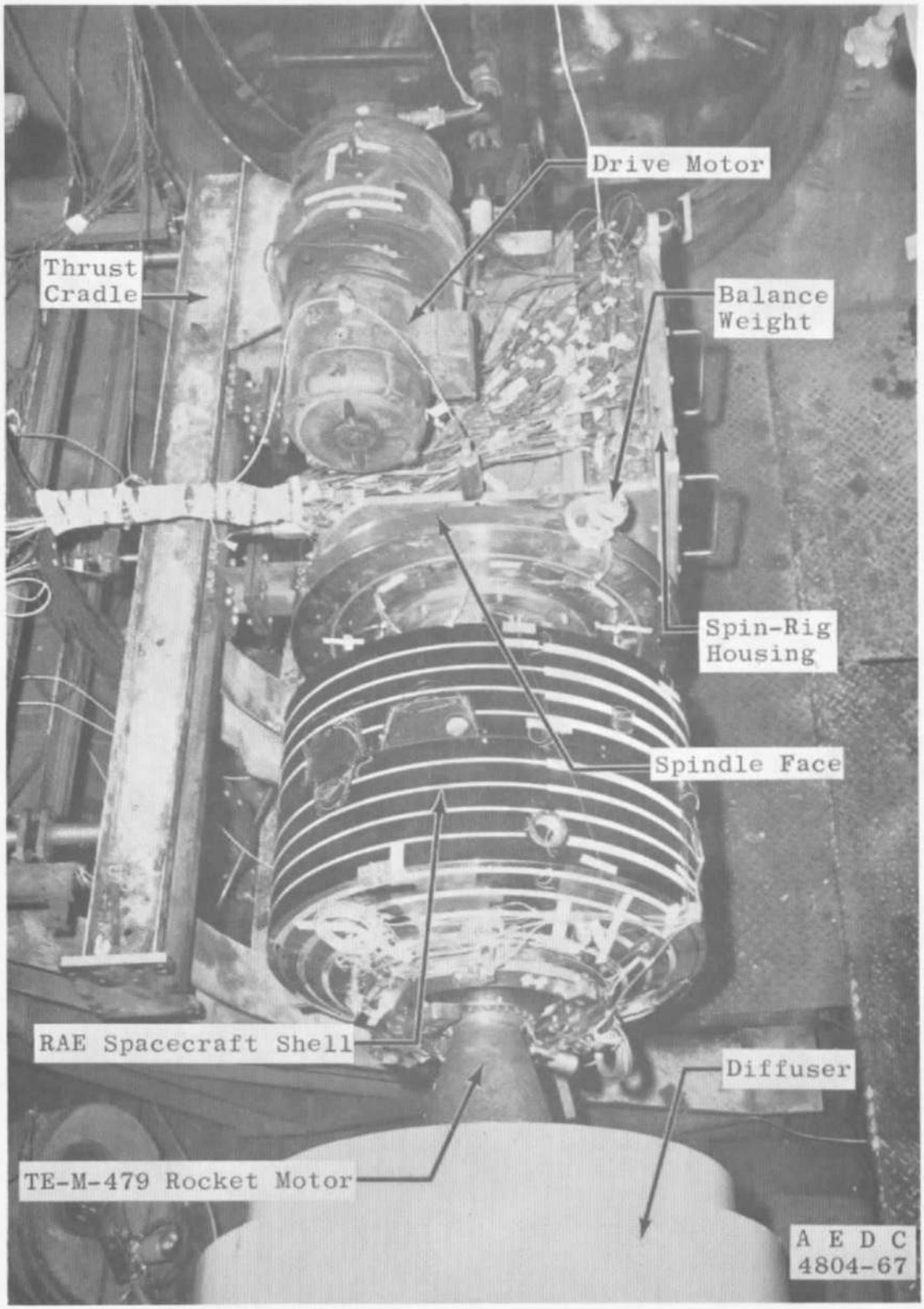

b. Photograph

Fig. 4 Continued

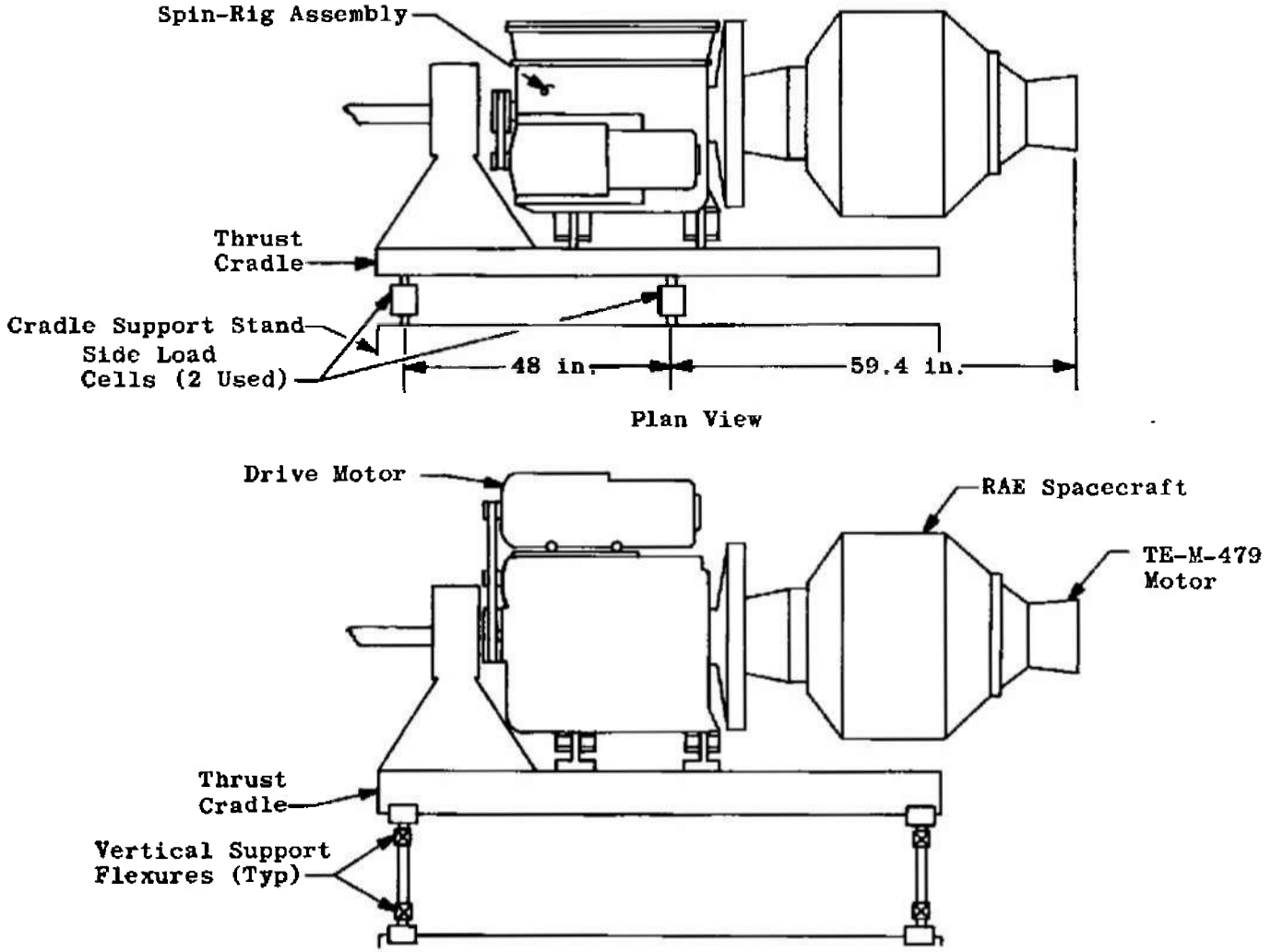

c. Detail

Fig. 4 Concluded

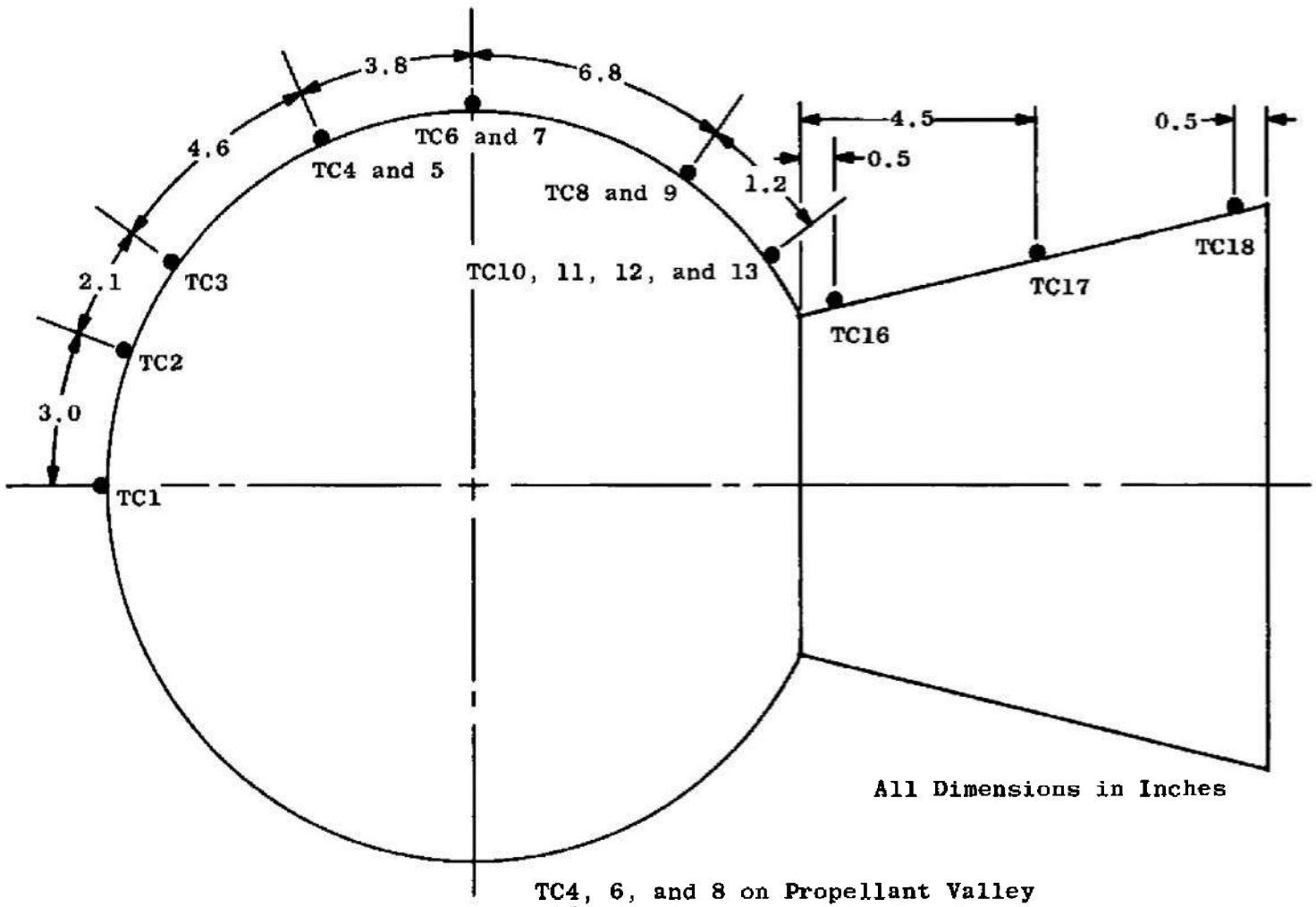

Fig. 5 Schematic Showing Thermocouple Locations on TE-M-479 Rocket Motor

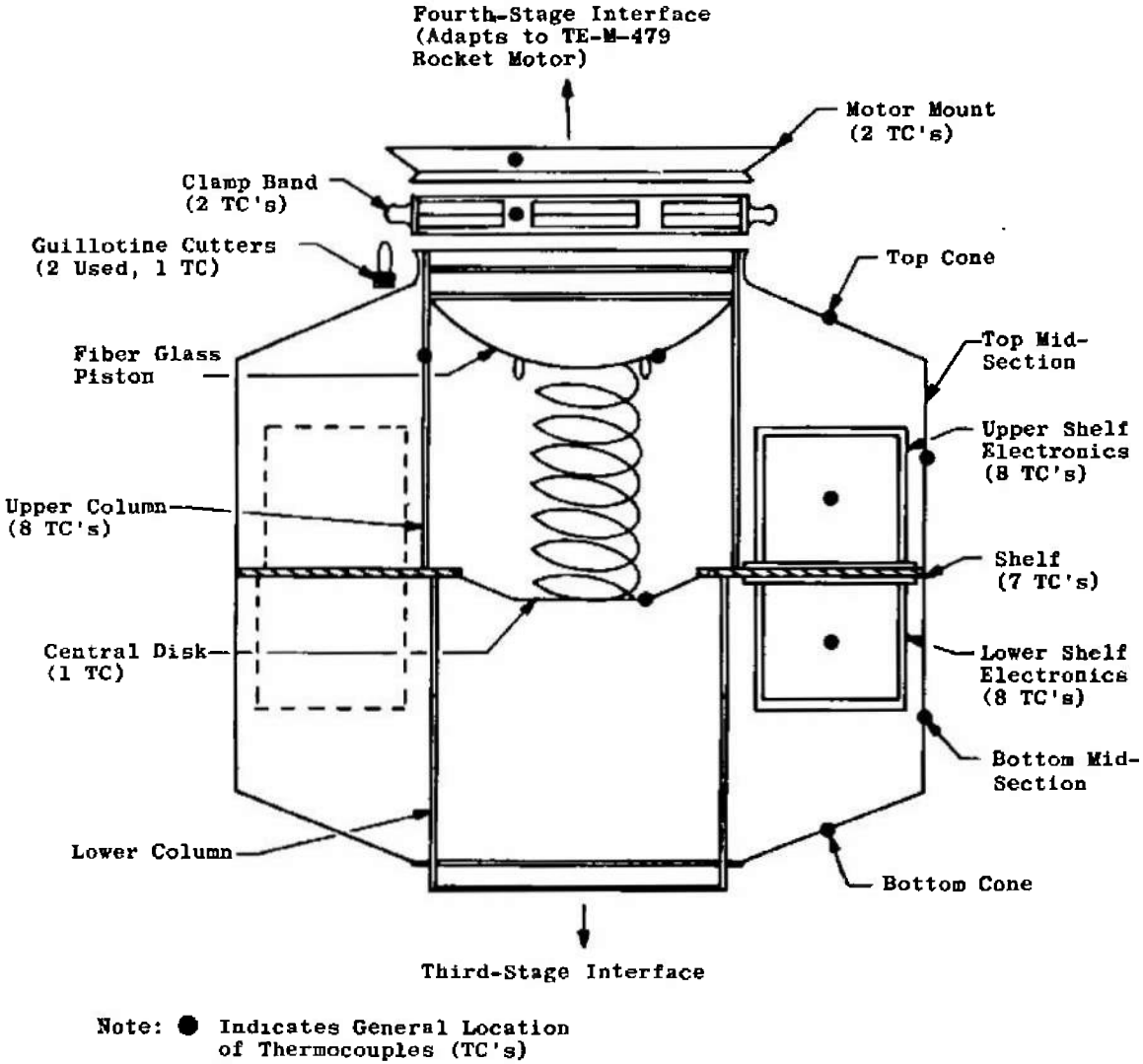

Fig. 6 Schematic Showing Thermocouple Locations on RAE Spacecraft

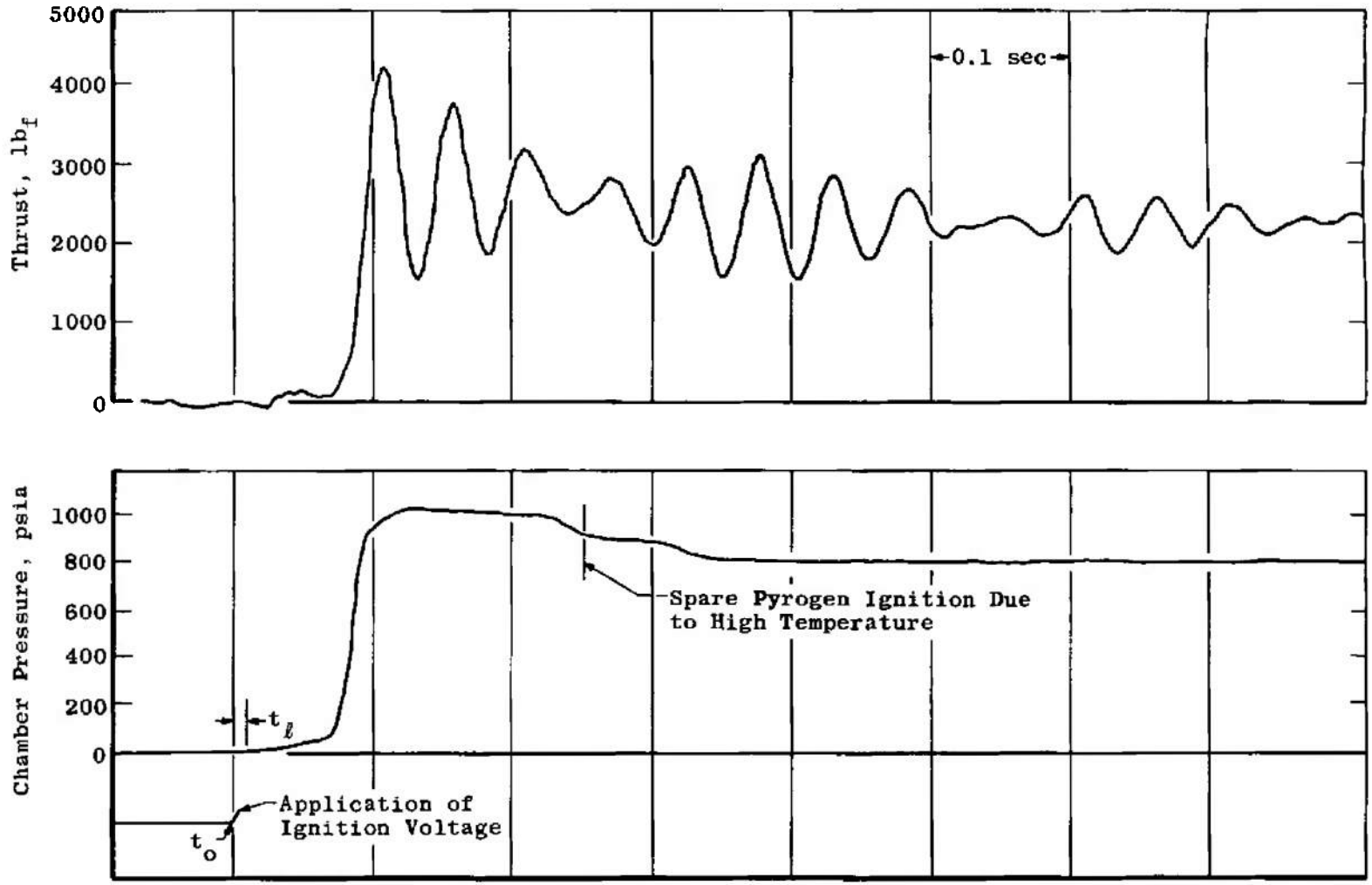

Fig. 7 Analog Trace of Typical Ignition Event (Motor S/N 7)

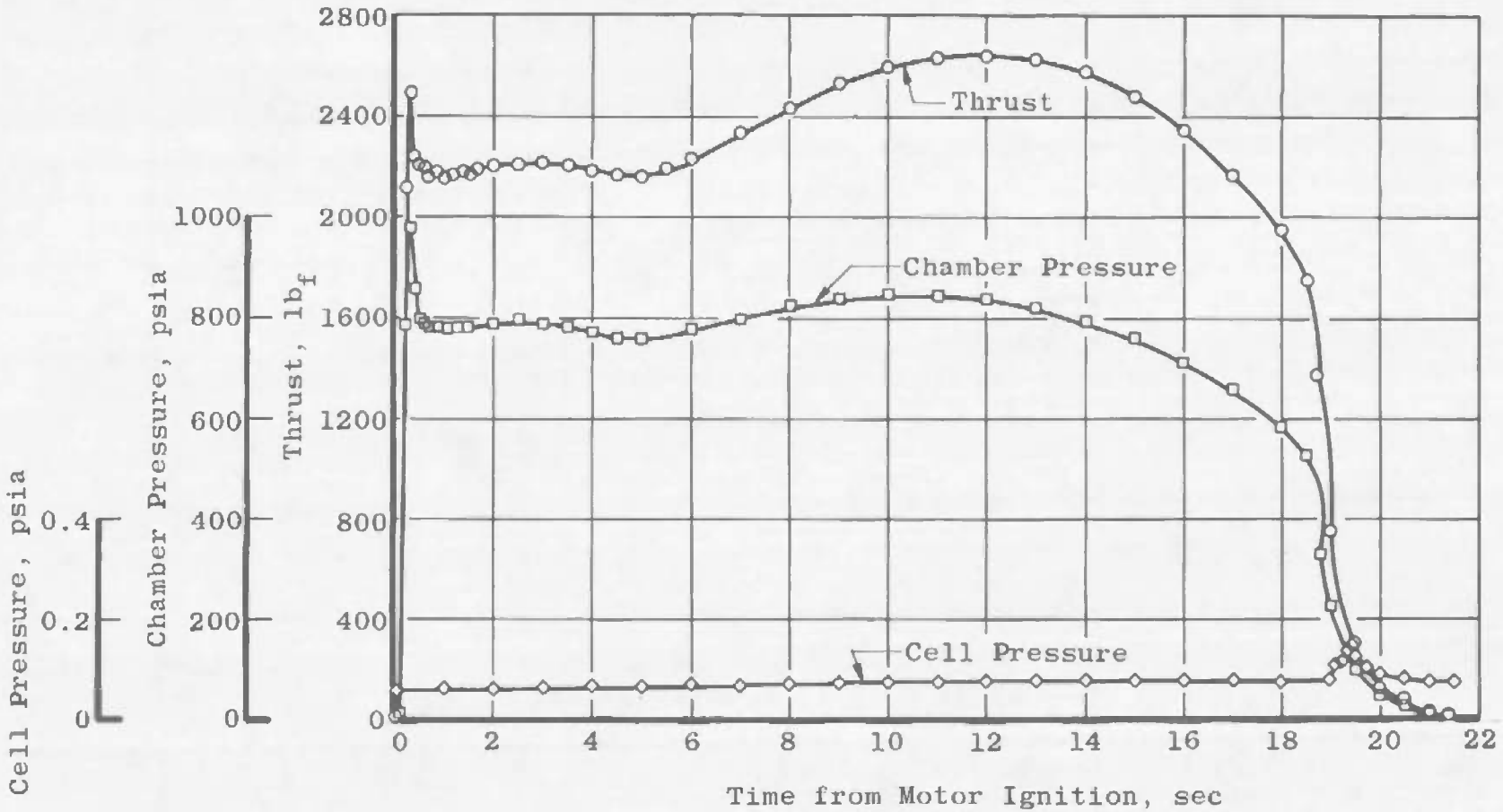

a. Motor S/N 7 (Temperature Conditioned at 40°F)

Fig. 8 Variation of Thrust, Chamber Pressure, and Test-Cell Pressure during Motor Burn Time

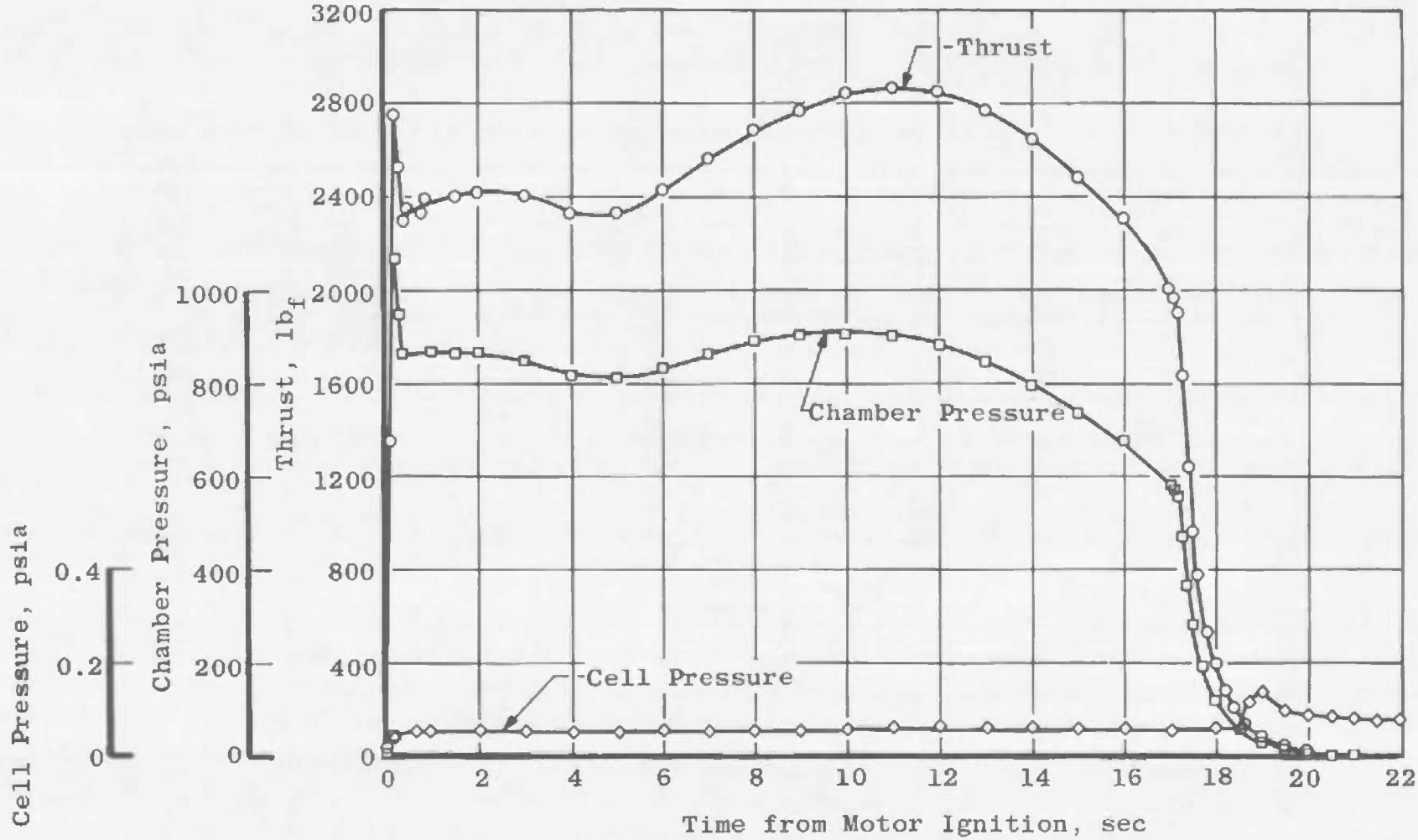

b. Motor S/N 10 (Temperature Conditioned at 90°F)

Fig. 8 Concluded

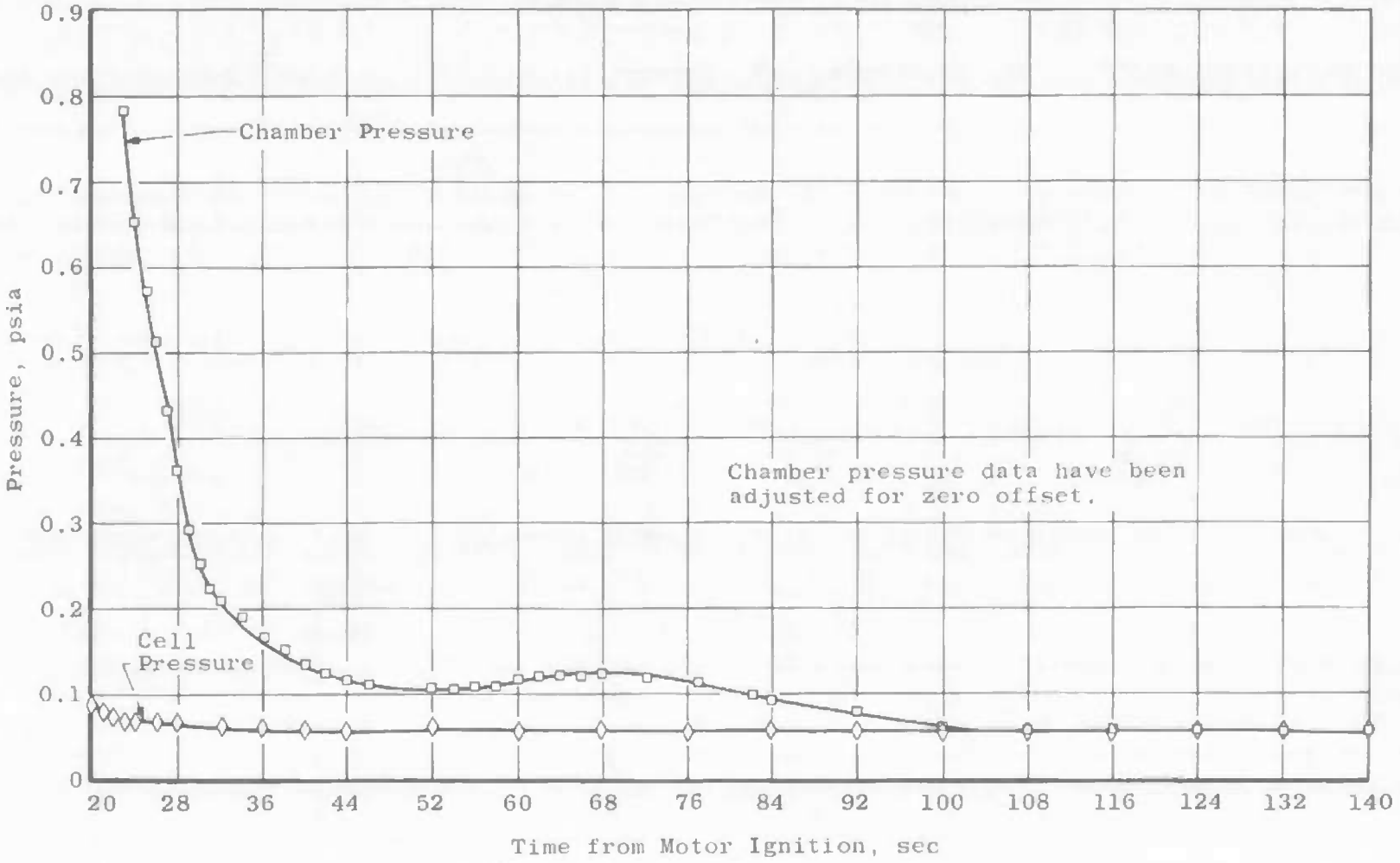

a. Motor S/N 7 (Temperature Conditioned at 40°F)

Fig. 9 Comparison of Low-Range Chamber Pressure and Test Cell Pressure during Motor Burn Time

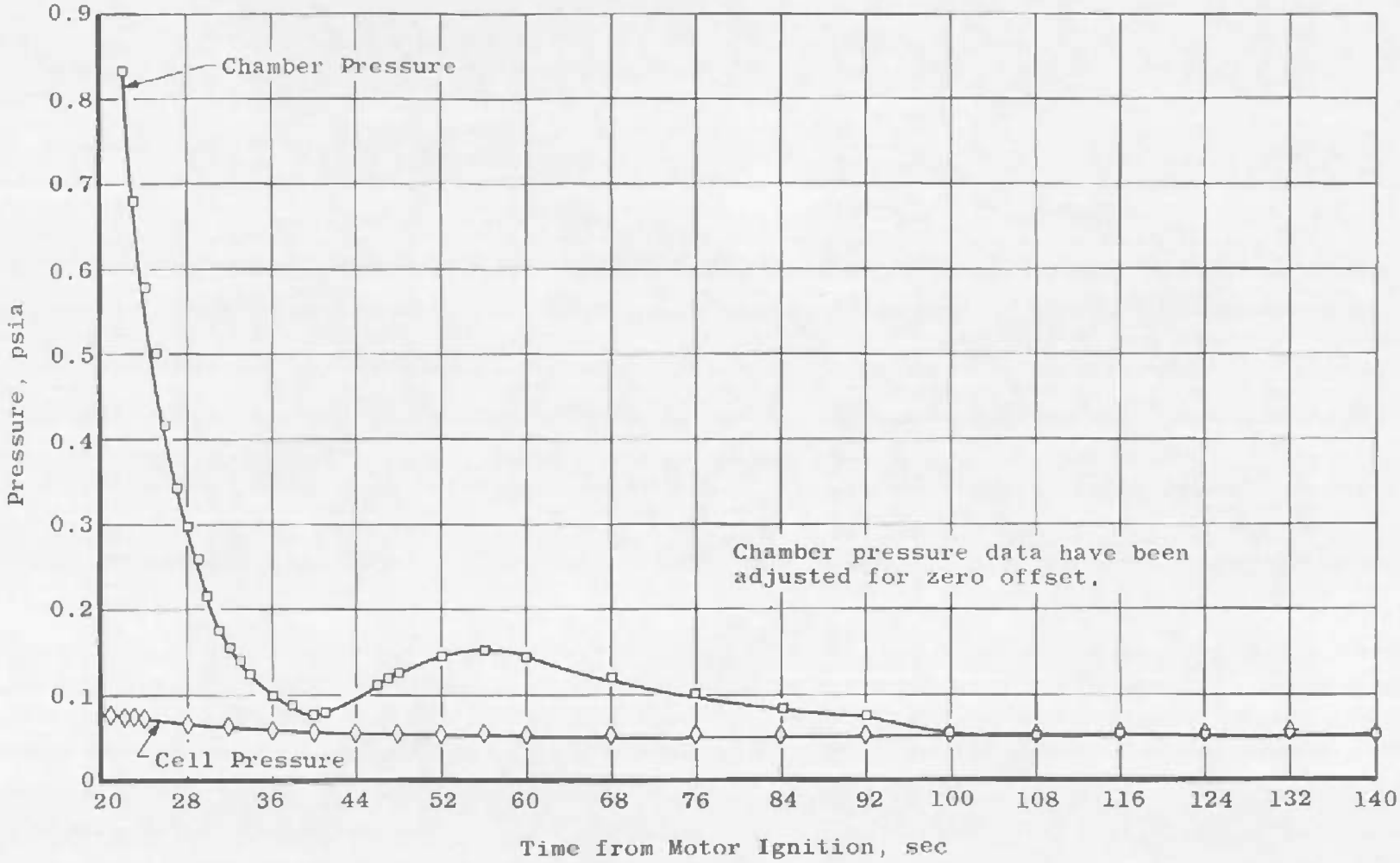

b. Motor S/N 10 (Temperature Conditioned at 90°F)

Fig. 9 Concluded

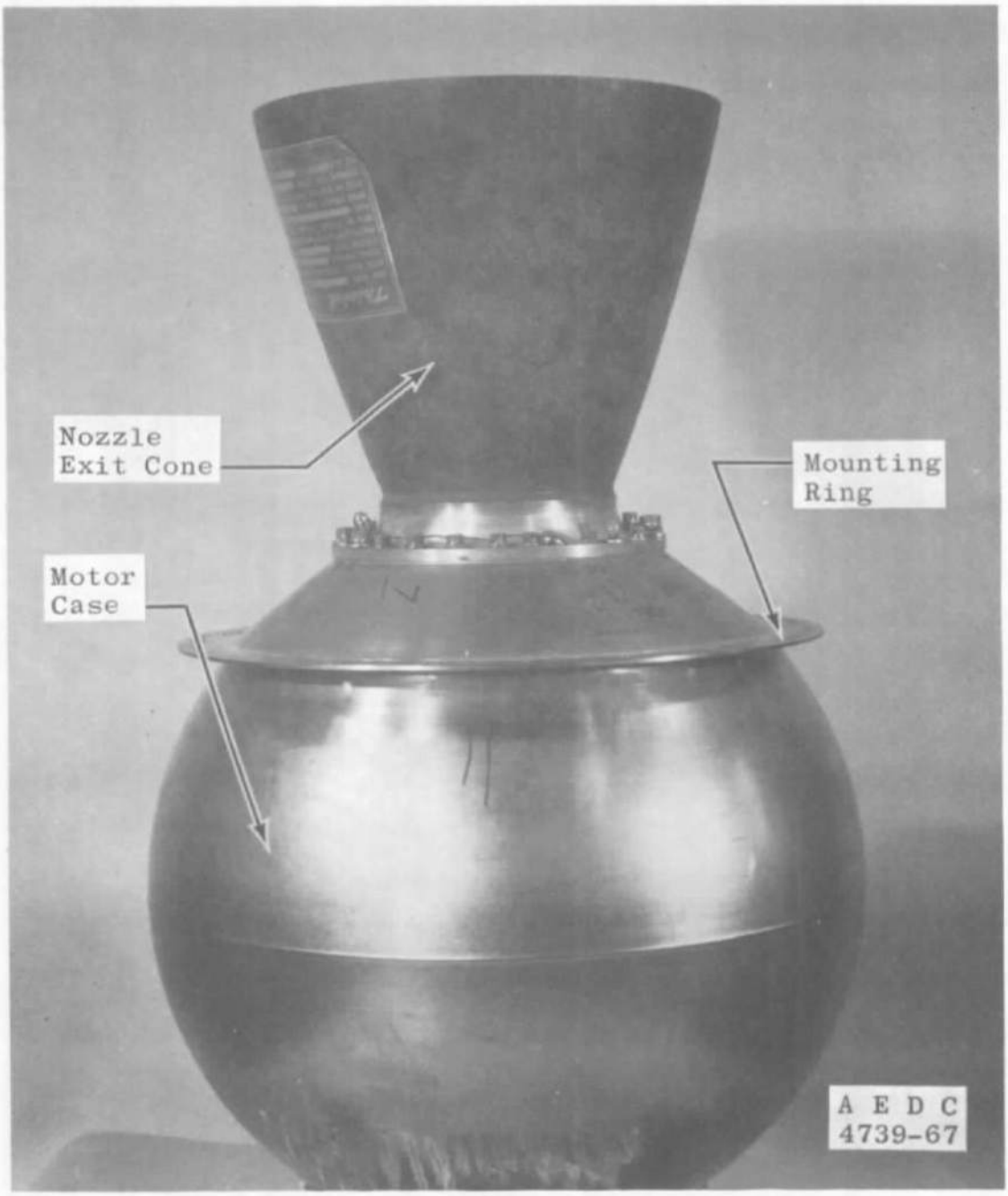

a. Exterior

Fig. 10 Photogrophs Showing Typicol Post-Fire Condition of TE-M-479 Rocket Motor (Motor S/N 7)

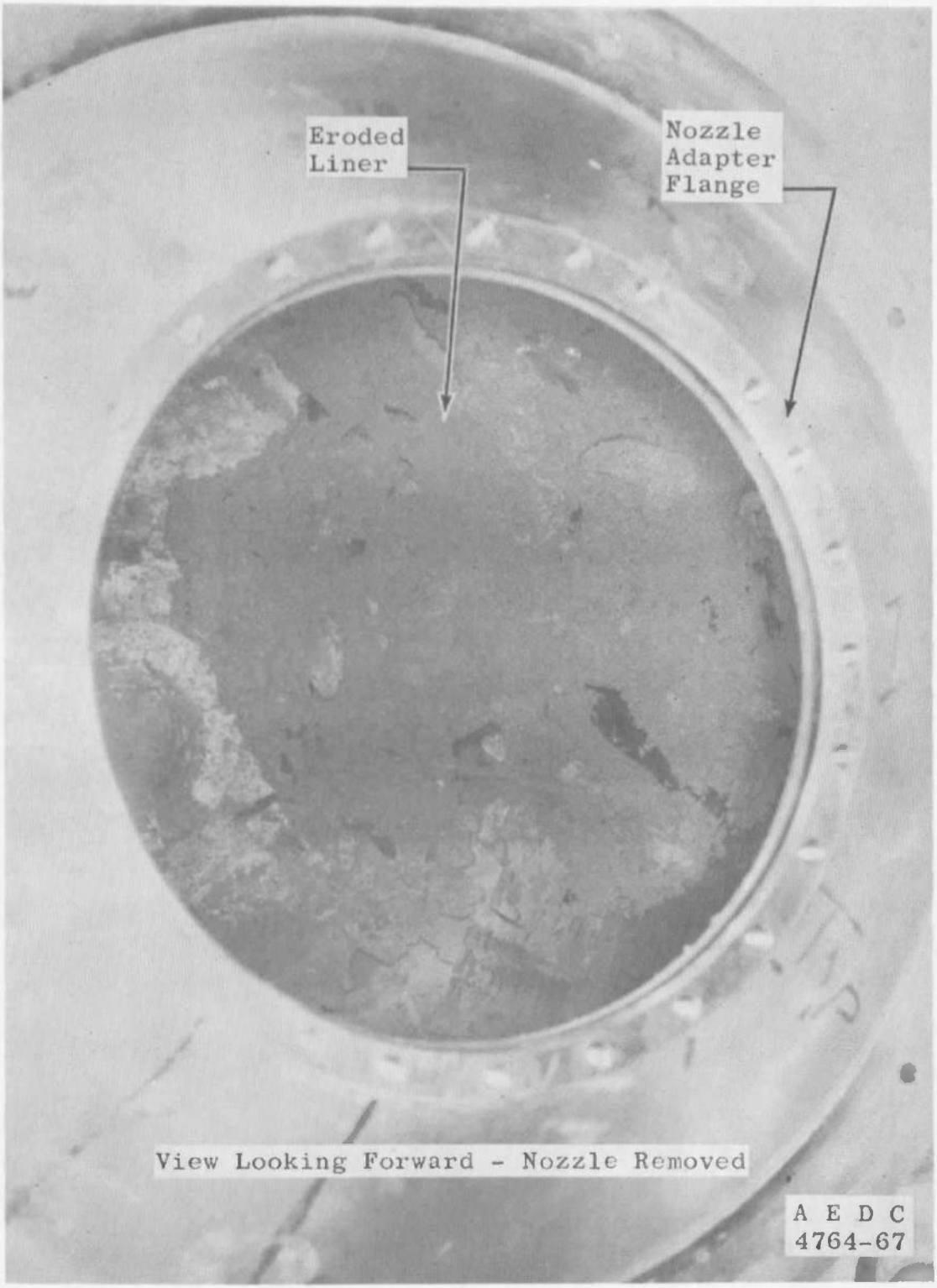

b. Interior

Fig. 10 Concluded

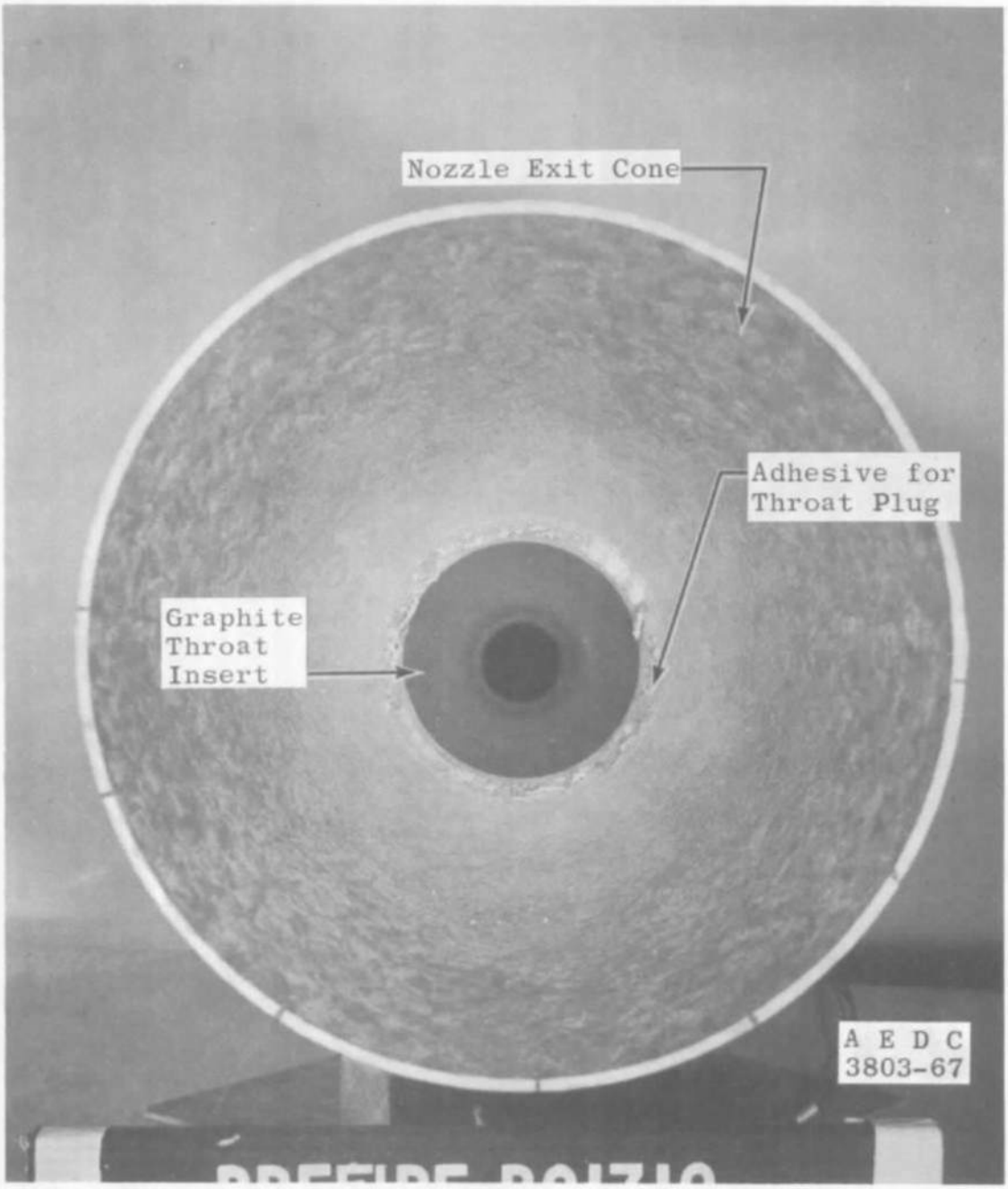

a. Pre-Fire

Fig. 11 Typical Pre- and Post-Fire Condition of Nozzle Exit Cone (Motor S/N 10)

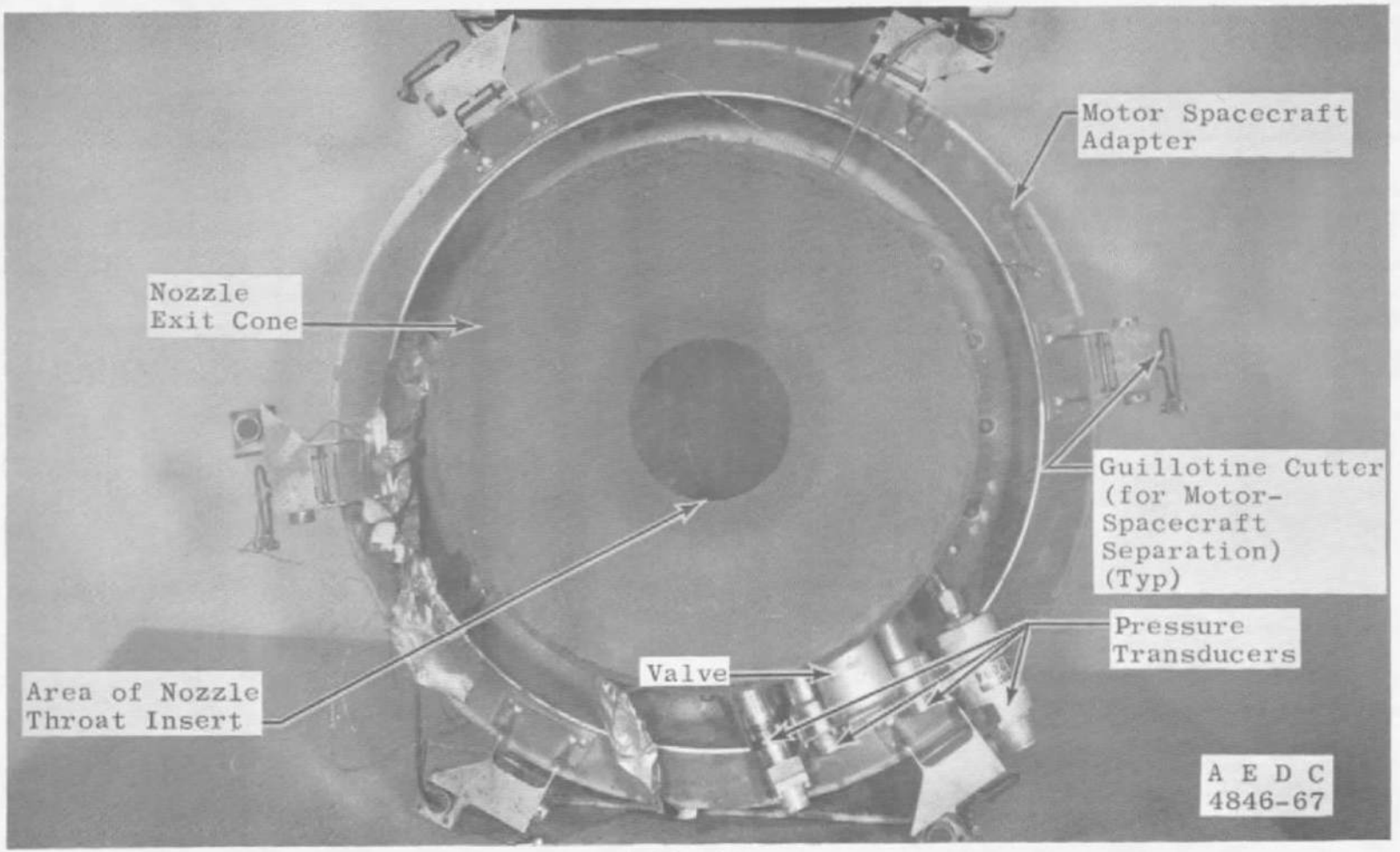

b. Post-Fire

Fig. 11 Concluded

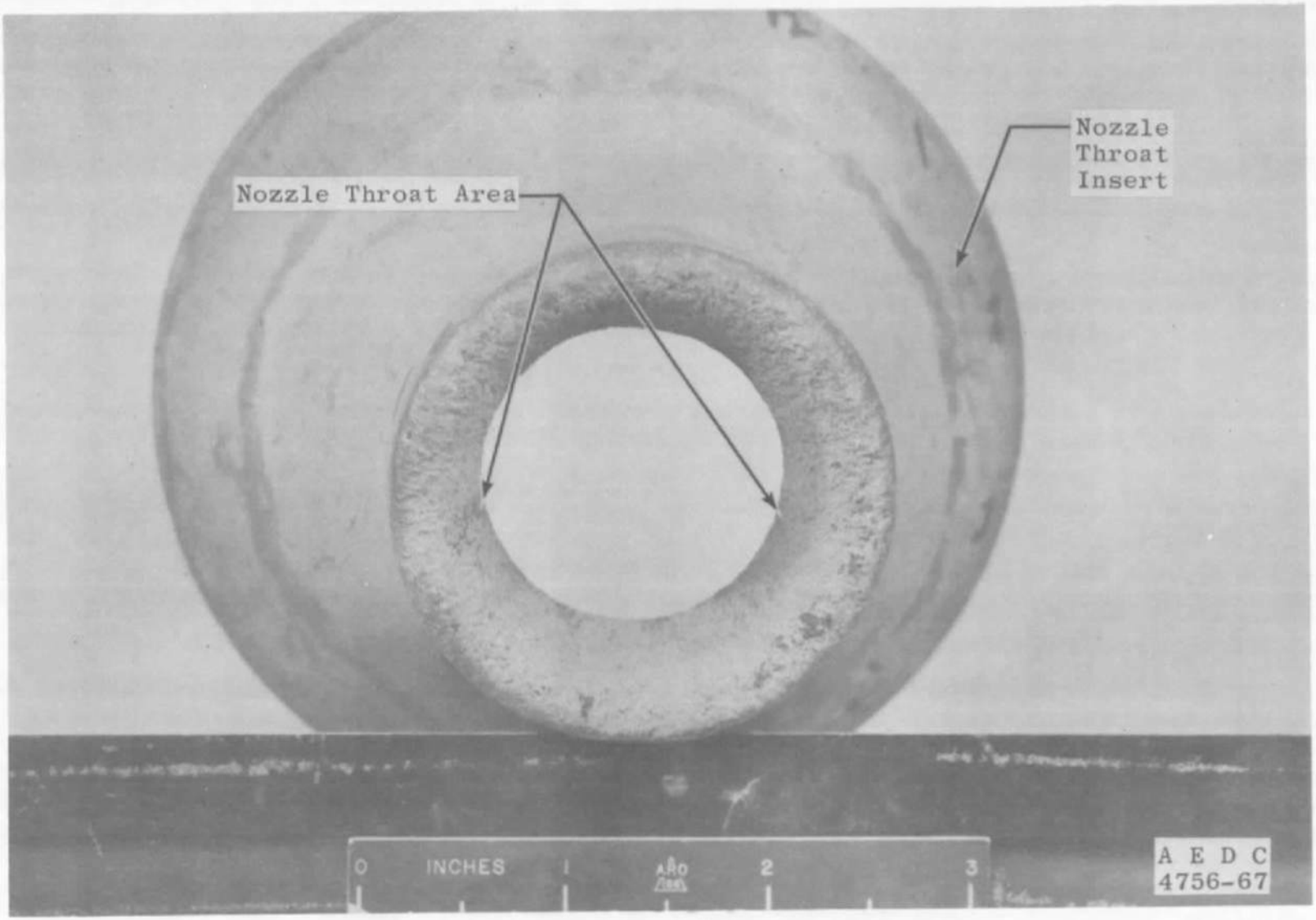

a. Motor S/N 7

Fig. 12 Post-Fire Condition of Nozzle Throat Inserts

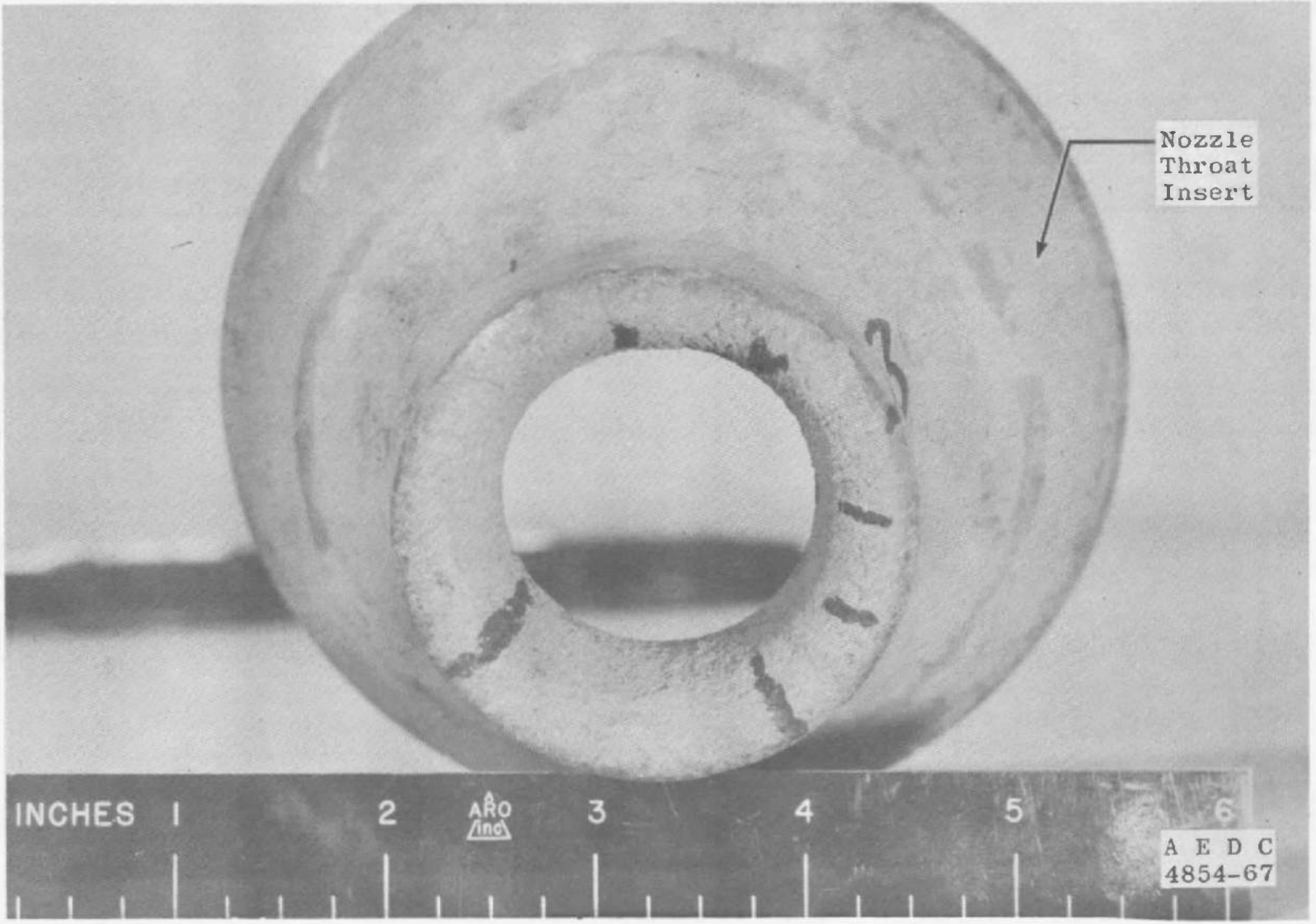

b. Motor S/N 10

Fig. 12 Concluded

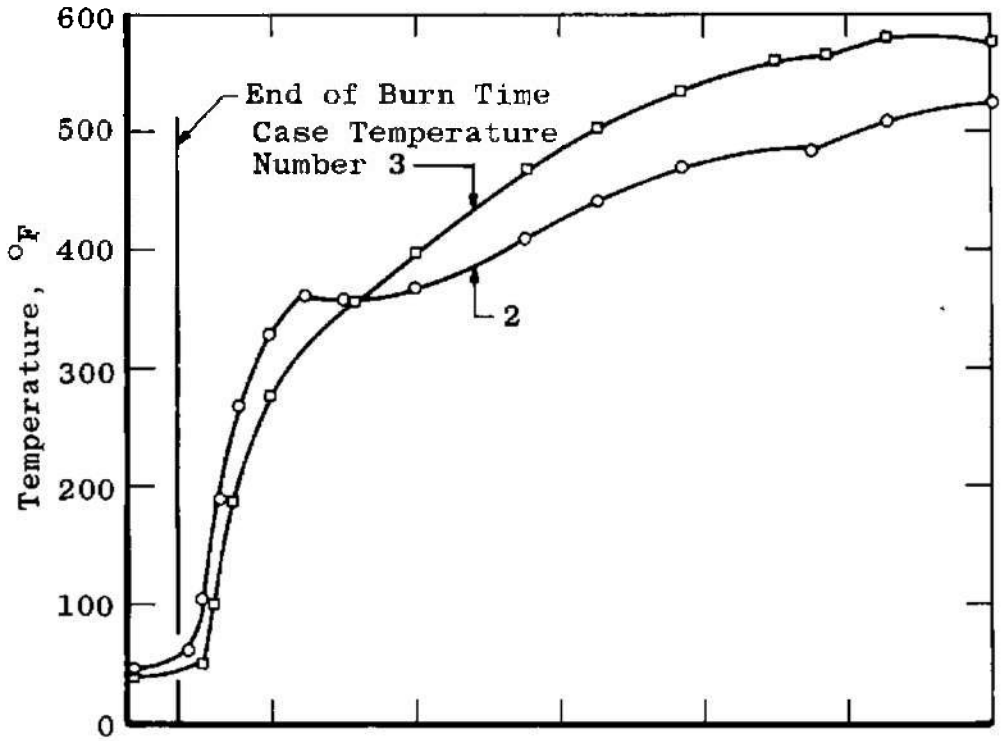

a. Motor S/N 7

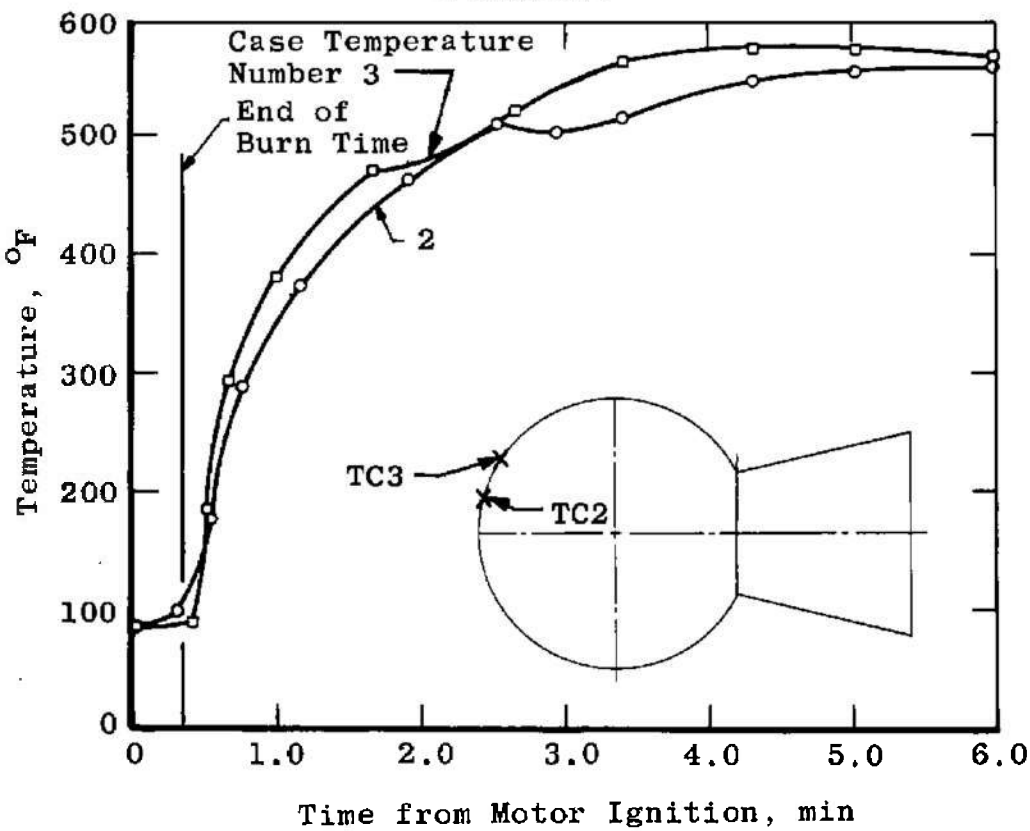

b. Motor S/N 10

Fig. 13 Time Variation of Motor Case (Forward) Temperatures

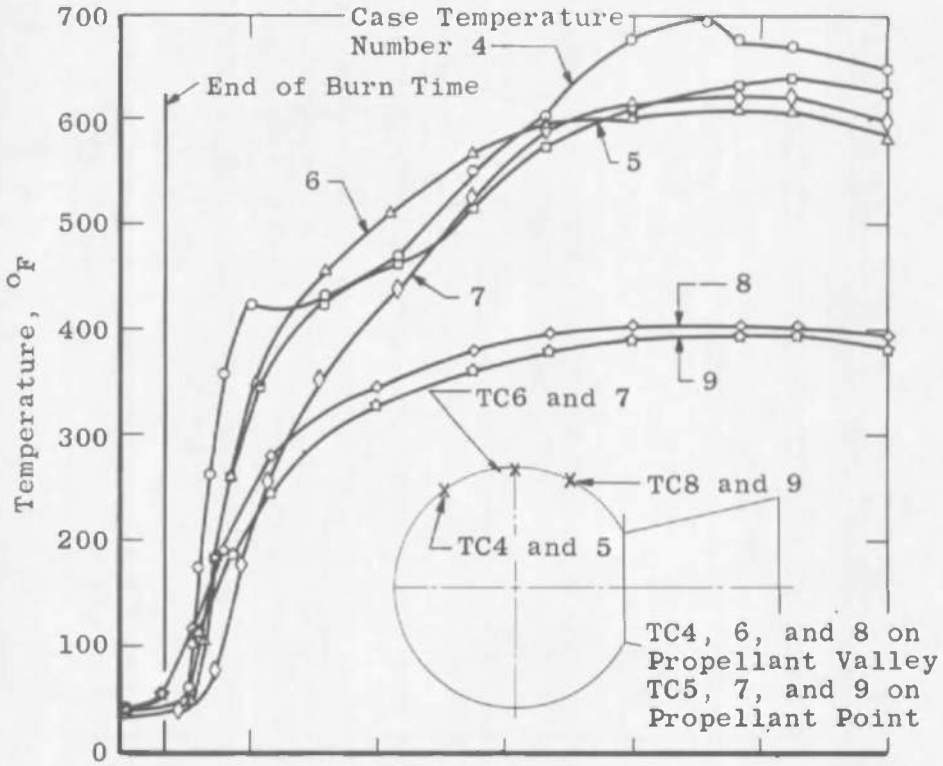

a. Motor S/N 7

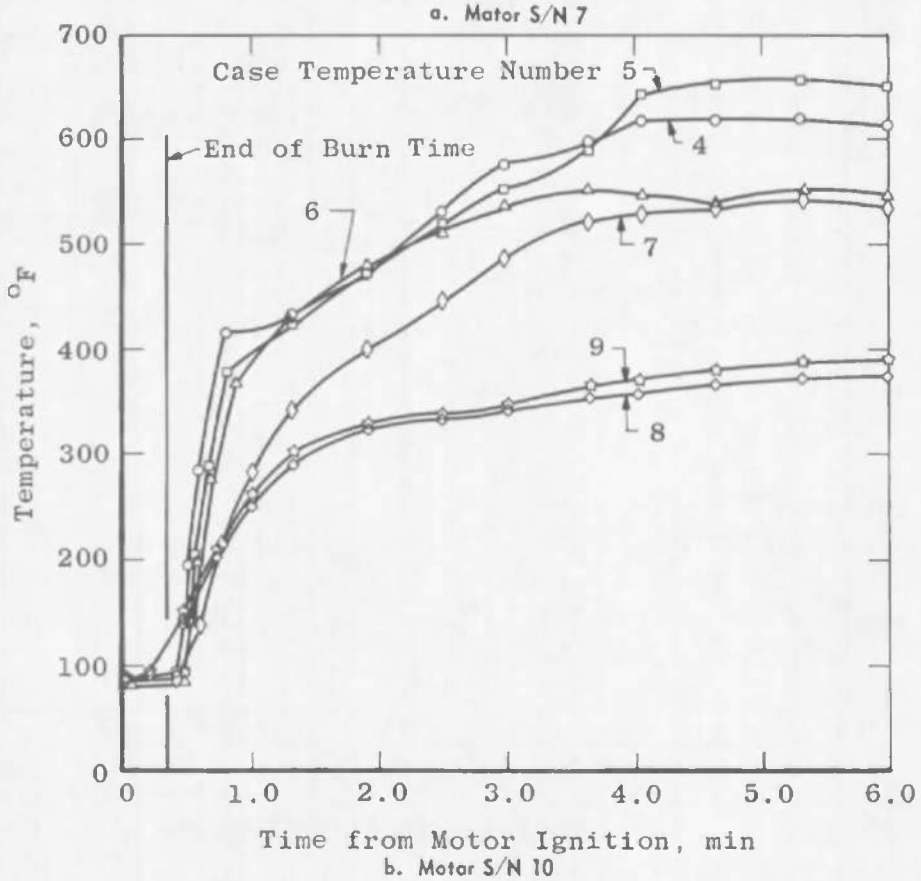

b. Motor S/N 10

Fig. 14 Time Variation of Motor Case (Central) Temperatures

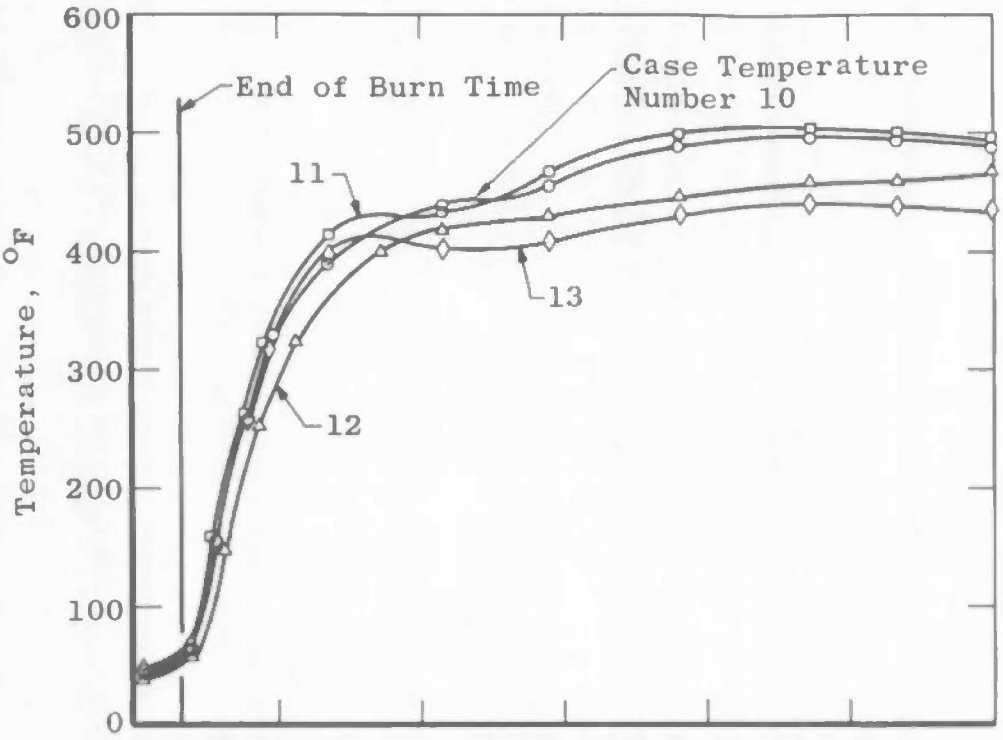

a. Motor S/N 7

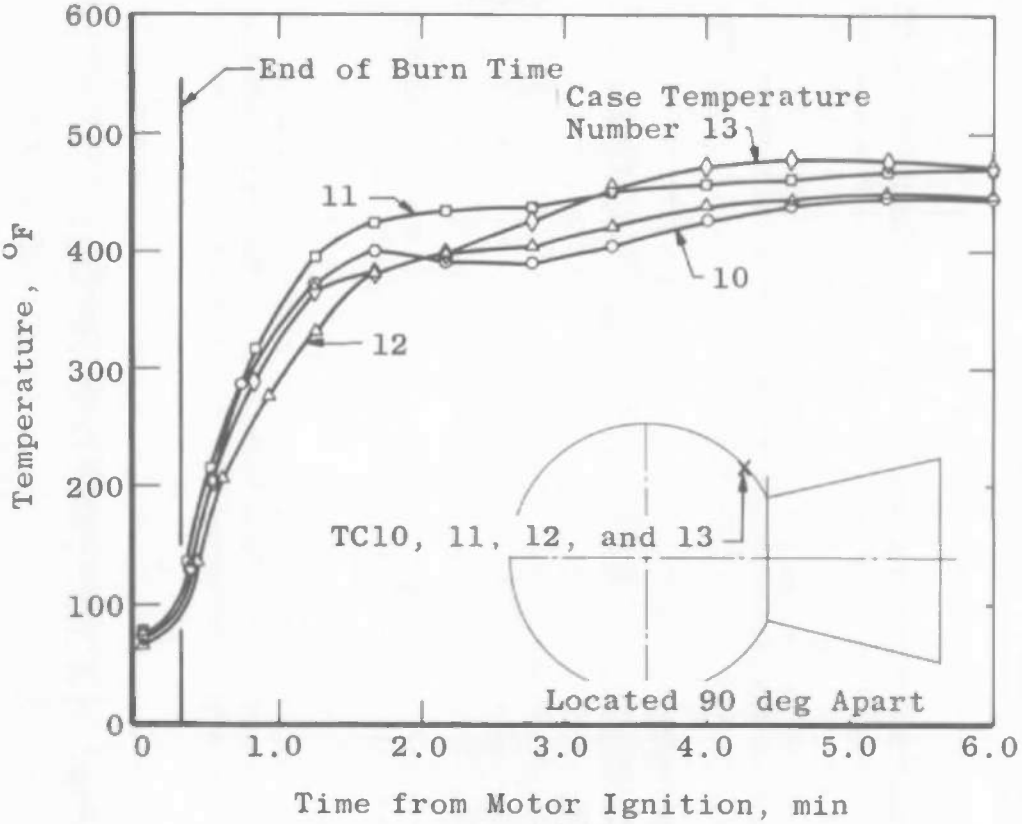

b. Motor S/N 10

Fig. 15 Time Variation of Motor Case (Aft) Temperatures

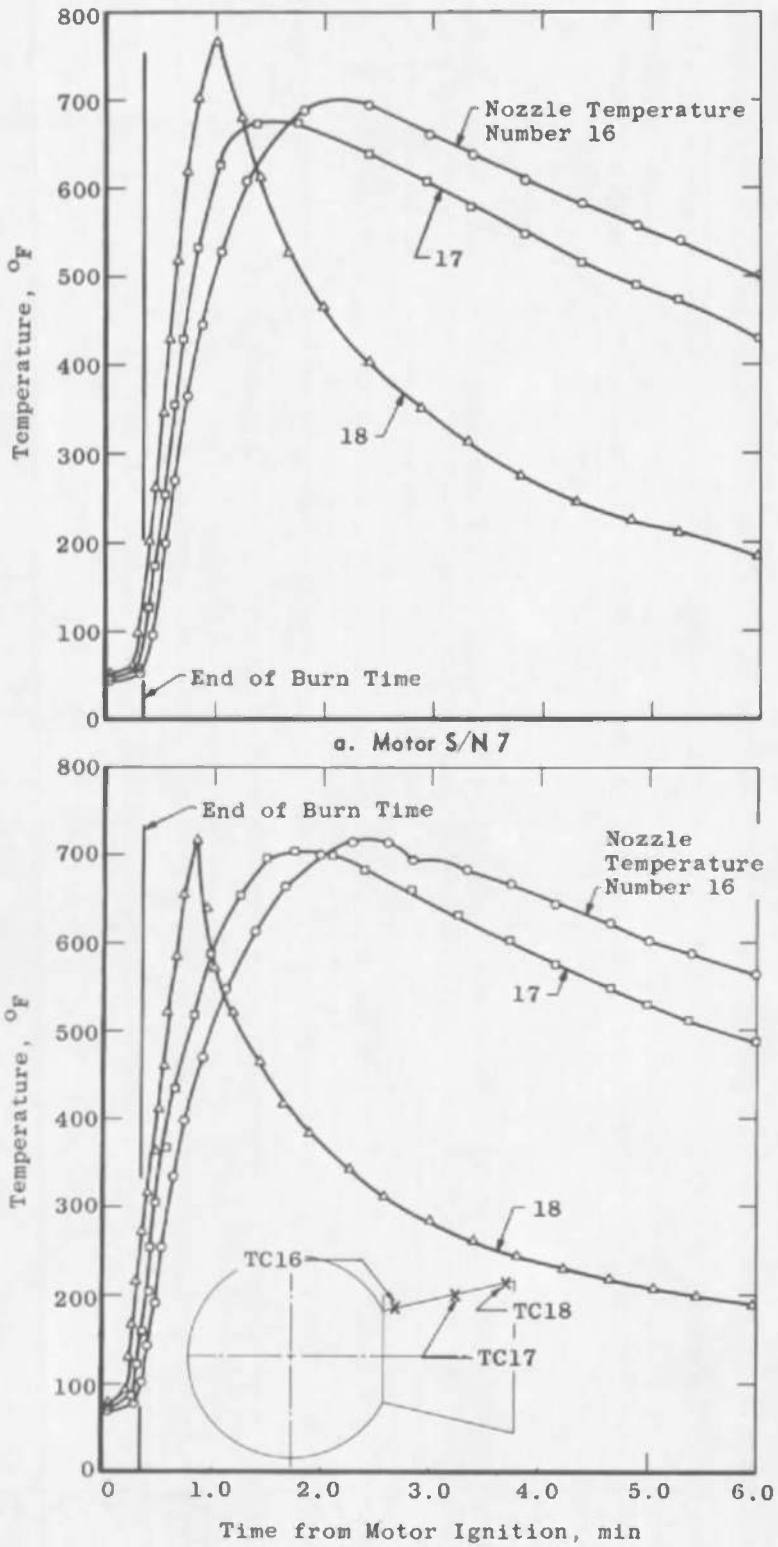

a. Motor S/N 7

b. Motor S/N 10

Fig. 16 Time Variation of Nozzle Temperatures

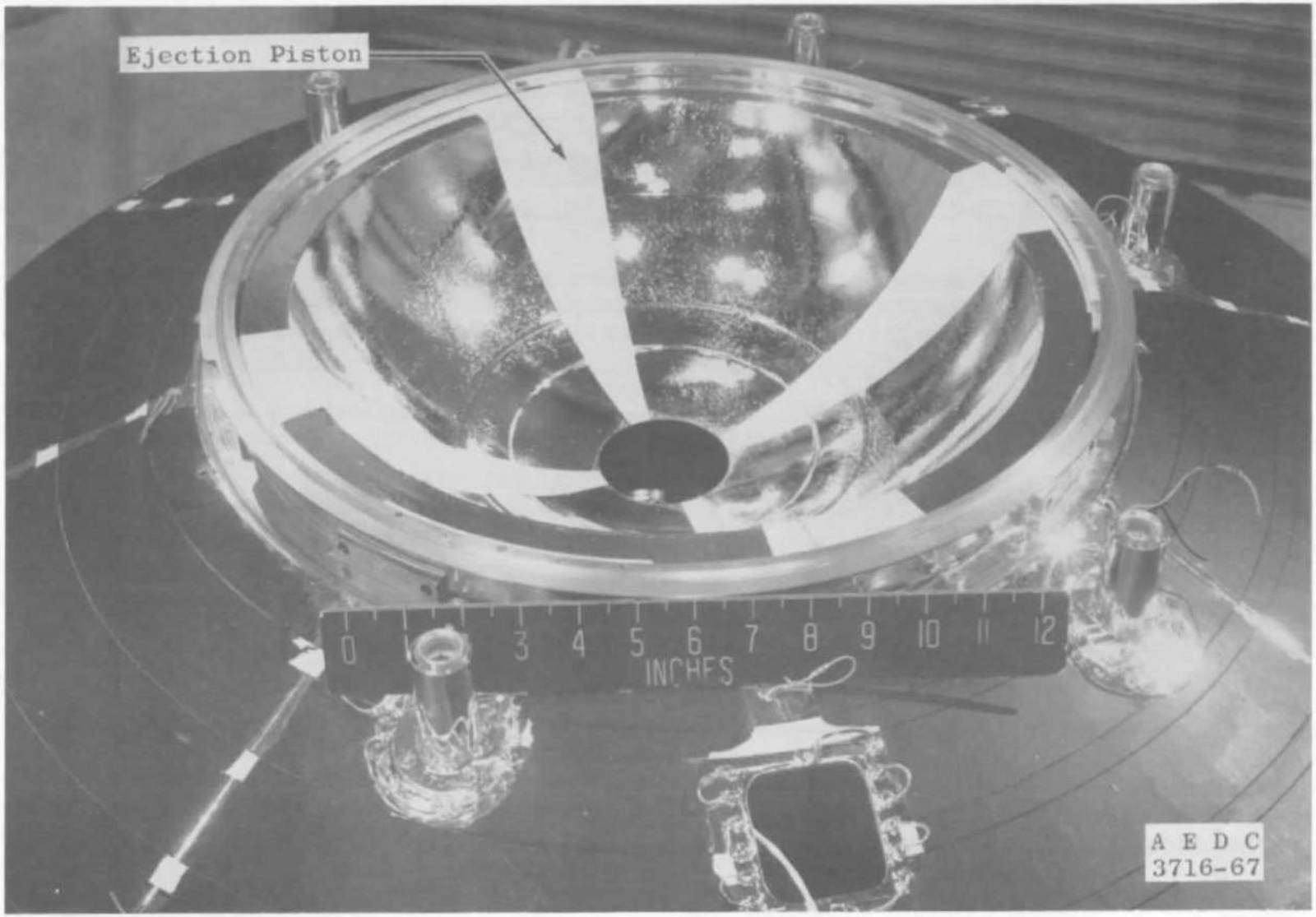

a. Pre-Fire

Fig. 17 Pre- and Post-Fire Condition of Ejector Piston for Motor S/N 7 Firing

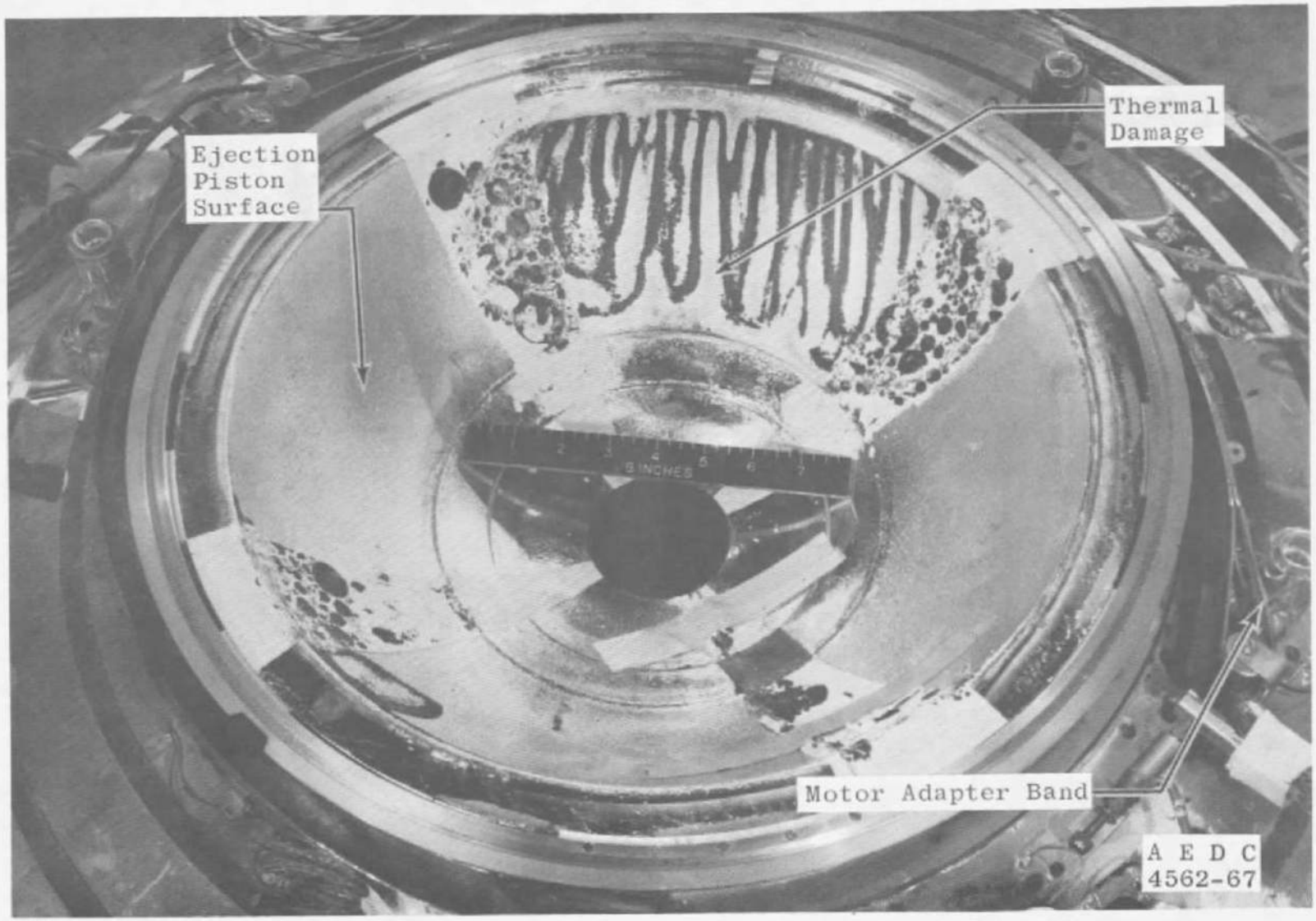

b. Post-Fire

Fig. 17 Concluded

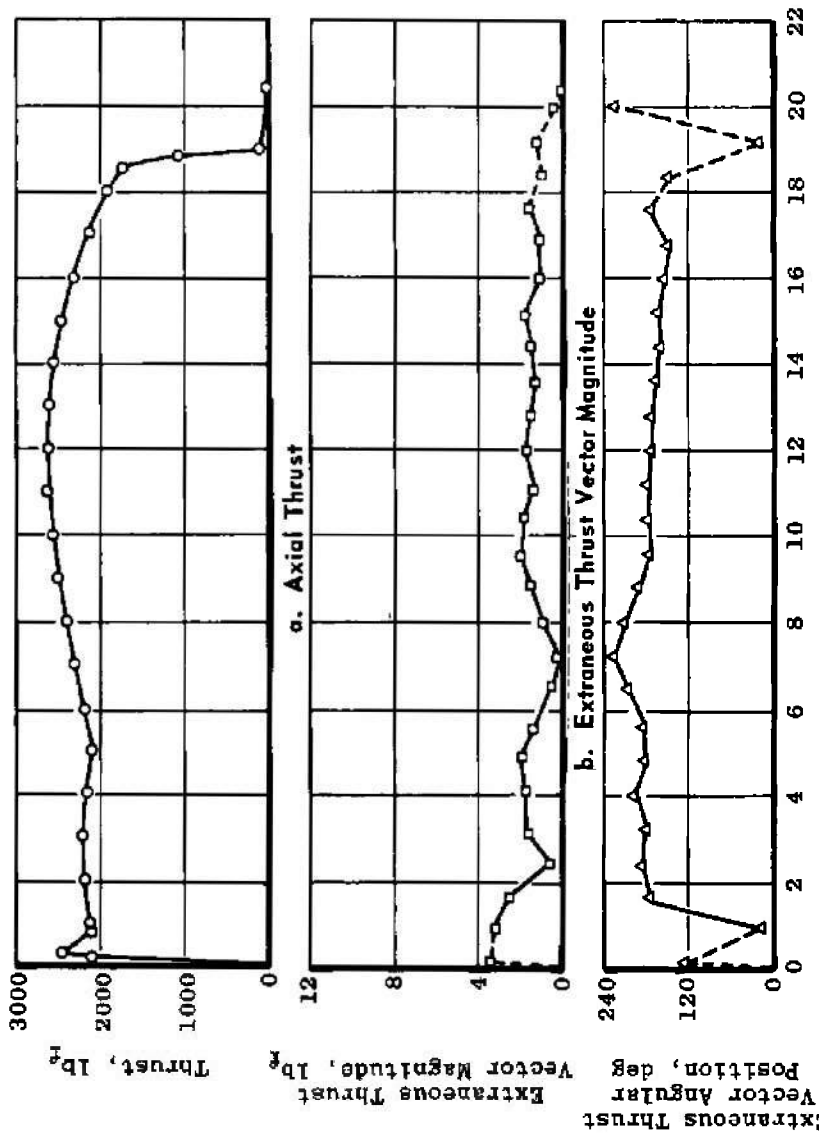

Fig. 18 Time Variation of Magnitude and Angular Position of Extraneous Thrust Vector during Motor Operation for Motor S/N 7

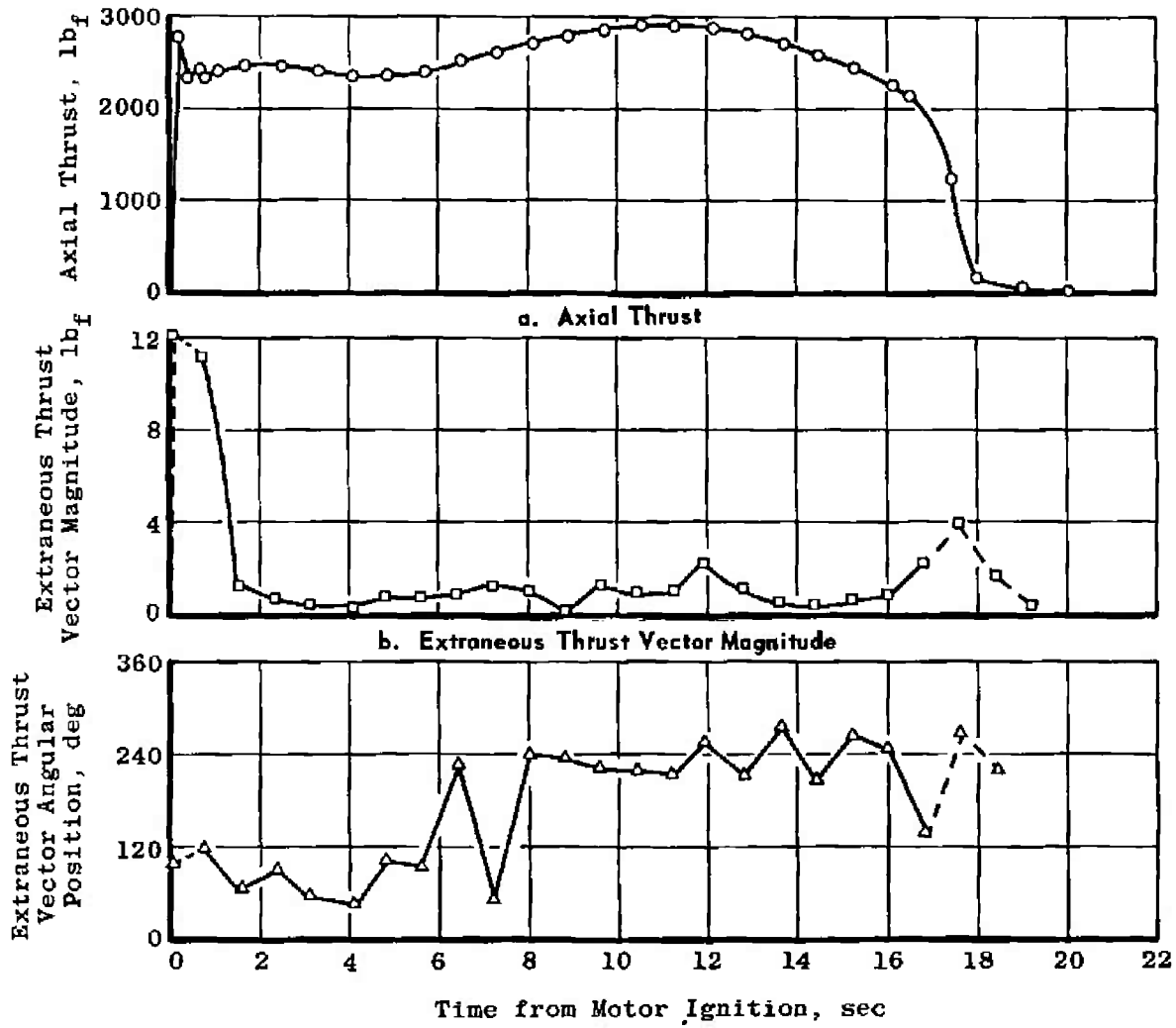

c. Extraneous Thrust Vector Angular Position

Fig. 19 Time Variation of Magnitude and Angular Position of Extraneous Thrust Vector during Motor Operation for Motor S/N 10

TABLE I
INSTRUMENTATION DESCRIPTION

Parameter	Estimated Measurement Uncertainty*		Measuring Device	Range of Measuring Device	Recording Device	Method of System Calibration
	Steady-State at Operating Level	Integral, percent				
Axial Force, lb_f	±0.32 percent	---	Bonded Strain-Gage-Type Load Cells (2 used)	0 to 5000 lb_f	Millivolt-to-Frequency or Digital Converter onto Magnetic Tape	Deadweight
Total Impulse, lb_f-sec	---	±0.31				
Motor Chamber Pressure, psia	±0.36 percent	---	Bonded Strain-Gage-Type Transducers (2 used)	0 to 1000 psia		Electrical
Chamber Pressure Integral, psia-sec	---	±0.35				
Low-Range Chamber Pressure, psia	±1.0 percent	---		0 to 5.0 psia		
Test Cell Pressure, psia	±1.26 percent	---	Unbonded Strain-Gage-Type Tranducers (3 used)	0 to 1.0 psia		
Test Cell Pressure, Integral, psia-sec	---	±1.21				
Time Interval, msec	±5 msec	---	Synchronous Timing Line Generator	---	Photographically Recording Galvanometer-Type Oscillograph	Compare with 60 cps
Temperature, °F	±5°F	---	Thermocouples	0 to 600°F	Digital Millivoltmeter onto Magnetic Tape	Known Millivolt Source and NBS Temperature Tables
Weight, lb_m	±0.020 lb_m	---	Beam Balance Scales	0 to 400 lb_m	Visual Readout	Periodic Deadweight Calibration
Extraneous Thrust Vector, lb_f	See Appendix III					

*All uncertainties are stated at an estimated two standard deviation level.

TABLE II
SUMMARY OF MOTOR PHYSICAL DIMENSIONS

Test Number 1710—	01	02
Motor S/N	7	10
Test Date	3/24/67	3/31/67
AEDC Pre-Fire Motor Weight, lb_m[1]	173.454	173.344
AEDC Post-Fire Motor Weight, lb_m[1]	18.172	17.813
AEDC Expended Mass, lb_m	155.282	155.531
Manufacturer's Stated Propellant Weight, lb_m	153.14	153.40
Nozzle Throat Area, $in.^2$		
Pre-Fire	1.483	1.478
Post-Fire	1.820	1.833
Percent Change from Pre-Fire Measurement	+22.7	+24.0
Nozzle Exit Area, $in.^2$		
Pre-Fire	88.993	90.010
Post-Fire	89.235	89.478
Percent Change from Pre-Fire Measurement	-0.84	-0.59
Nozzle Area Ratio		
Pre-Fire	60.01	60.90
Post-Fire	49.03	48.82
Average	54.90	54.86

[1]Does not include igniter weight

TABLE III
SUMMARY OF MOTOR PERFORMANCE

Test Number RC1710	01	02
Motor S/N	7	10
Test Date	3/24/65	3/31/65
Cell Temperature at Ignition, °F	47	100
Ignition Lag Time (t_ℓ), [1] sec	0.010	0.011
Action Time (t_a), [1] sec	19.5	18.2
Full-Duration Burn Time (t_{f_b}), [1] sec	21.4	20.2
Simulated Altitude at Ignition, ft	124,000	127,000
Average Simulated Altitude during t_{f_b}, ft	118,000	123,000
Average Motor Spin-Rate during Firing, rpm	75.36	75.26
Measured Total Impulse (Based on t_a), lb_f-sec	44,117	44,329
Number of Channels Averaged	3	4
Maximum Deviation of Individual Channel from Average, percent	0	0.02
Measured Total Impulse (Based on t_{f_b}), lb_f-sec	44,266	44,473
Number of Channels Averaged	3	4
Maximum Deviation of Individual Channel from Average, percent	0	0.02
Chamber Pressure Integral (Average of Two Channels, Based on t_{f_b}), psia-sec	14,566	14,475
Maximum Deviation of Individual Channel from Average, percent	0.04	0.07
Cell Pressure Integral (Average of Three Channels, Based on t_{f_b}), psia-sec	1.5579	1.0586
Maximum Deviation of Individual Channel from Average, percent	0.24	0.28
Vacuum Total Impulse, lb_f-sec		
Based on t_a	44,239	44,424
Based on t_{f_b}	44,406	44,583

TABLE III (Concluded)

Vacuum Specific Impulse (Based on t_a), lb_f-sec/lb_m		
Based on the Manufacturer's Stated Propellant Weight	288.88	289.60
Based on AEDC Measured Expended Mass	284.90	285.63
Vacuum Specific Impulse (Based on t_{f_b}), lb_f-sec/lb_m		
Based on the Manufacturer's Stated Propellant Weight	289.97	290.63
Based on AEDC Measured Expended Mass	285.97	286.65
Average Vacuum Thrust Coefficient (C_F) (Based on t_a and Average Pre- and Post-Fire Throat Area)	1.846	1.854
Maximum Motor Case Temperature, °F	691	654
Time of Occurrence of Maximum Motor Case Temperature (from Ignition), sec	263	290

[1]See Nomenclature for Definitions

APPENDIX III
CALIBRATION OF EXTRANEOUS THRUST VECTOR MEASURING SYSTEM TO DETERMINE SYSTEM ACCURACY

In order to determine the accuracy of extraneous thrust vector measurement using the spin-technique, a spin-calibration of the test configuration was accomplished. A description of the calibration technique used for the test reported herein is presented in the following sections.

INSTALLATION

The spin-fixture was mounted on the thrust cradle with the spin axis aligned with the axial thrust column centerline. Forward and aft side load cells (0- to 100-lb_f) were mounted in the plane of the spin fixture horizontal centerline as shown in Fig. 4c. A stiffness check was made on the spin fixture-thrust cradle configuration which consisted of moving the assembly laterally off the mechanical null position a known amount and measuring the force exerted by the assembly on the side load cells.

A heavyweight mounting can, simulating the test motor/spacecraft configuration, was installed on the spin fixture and its centerline concentrically aligned with the fixture spin axis.

The entire system was aligned so that no horizontal force was indicated by either the forward or aft side load cell (mechanical null position).

CALIBRATION PROCEDURE

A stand static calibration to determine system response to static, lateral loads was first accomplished. This consisted of applying known lateral forces (tension and compression) to the mounting can with and without an axial load of 2700 lb_f applied to the system. The lateral loads were applied normal to the thrust axis in the area of expected extraneous thrust vector occurrence. A comparison of measured and applied force is presented in Fig. III-1. The measured force was, in all cases, greater than the applied force because, as the system is forced away from its mechanical null position, a weight component of the system, greater than the flexure restoring force, was measured in addition to, and in the same direction as, the applied force.

After the stand static calibration, the mounting can was rotated at 75 rpm about its axial centerline and balanced to a degree where total side force produced by system unbalance was less than 5 lb_f. A dynamic (spin) calibration was then performed. This calibration consisted of placing accurately measured weights at several angular locations on the mounting can surface to produce a known force as a function of spin rate:

$$F = mr\omega^2$$

where:

F = centrifugal force, lb_f,

m = applied mass, lb_m,

r = radius of can, ft and

ω = rotational speed, rad/sec

Two masses (nominally 1 and 2 lb_m) were attached to the can at three different angular locations (0, 60, and 120 deg). The calibration was conducted at both sea-level and altitude conditions, with and without axial load applied.

DATA ACQUISITION AND REDUCTION

Applied Force

The applied side force was determined from the relationship:

$$F = \frac{x}{x_o} \, m r_{(app)} \, \omega^2$$

where

$mr_{(app)}$ is the applied unbalance (product of applied mass and its radial distance), and ω is the rotational speed. The ratio $\left(\frac{X}{X_o}\right)$ is the magnification factor of forced vibration and is a function of the ratio of spin frequency (ω) to stand natural frequency (ω_n) as:

$$\frac{x}{x_o} = \frac{1}{\sqrt{\left[1 - \left(\frac{\omega}{\omega_n}\right)^2\right]^2 + \left(2\zeta \frac{\omega}{\omega_n}\right)^2}}$$

(The damping factor, ζ, was assumed to be zero.)

Measured Force

Side force data were recorded on magnetic tape during the calibration sequence. These data were then electronically filtered to remove all frequencies above the rotational frequency.

The side force magnitude (average of approximately 10 peaks) and angular location (from oscillograph recording as in Fig. III-2) were corrected for filter effects as outlined in Ref. 3.

The measured side-force (determined based on the stand static calibration results), after incorporating filter corrections, consisted of the force due to the applied unbalance and the residual dynamic force (balance result) in the system with no unbalance applied. A true measured side-force resulted when the residual force was vectorially subtracted from the measured side force.

RESULTS

Stand Static Calibration

Figure III-1 is a comparison of measured and applied static force for the calibration reported herein. Horizontal forces were applied in both tension (away from side load cells) and compression (toward side load cells) in a range from 0 to 35 lb_f both with and without an axial load applied to the stand. The effect of stand deflection of the measured force was the same both with and without axial load. The ratio of measured to applied static force was 1.022 in both cases.

Dynamic Calibration

Nominal unbalances of 30 and 50 in.-lb_m were applied at angular locations of 0, 60, and 120 deg while the system was at sea-level conditions. A nominal unbalance of 50 in.-lb_m located at 0 deg was applied for the calibration at a simulated altitude of approximately 120,000 ft.

A comparison of true measured and applied side force is presented in Fig. III-3. Since the true measured side force is an average of 10 peaks, an envelope of the averaged data points is presented and incorporated into the accuracy determination. The maximum deviation of ±0.15 lb_f was observed at an applied force of 4.94 lb_f; however, an additional deviation of ±0.11 lb_f was introduced when individual peaks were analyzed. The system accuracy based on estimated 1 standard deviation for the test reported herein was, therefore, ±0.27 lb_f at the steady-state side force level.

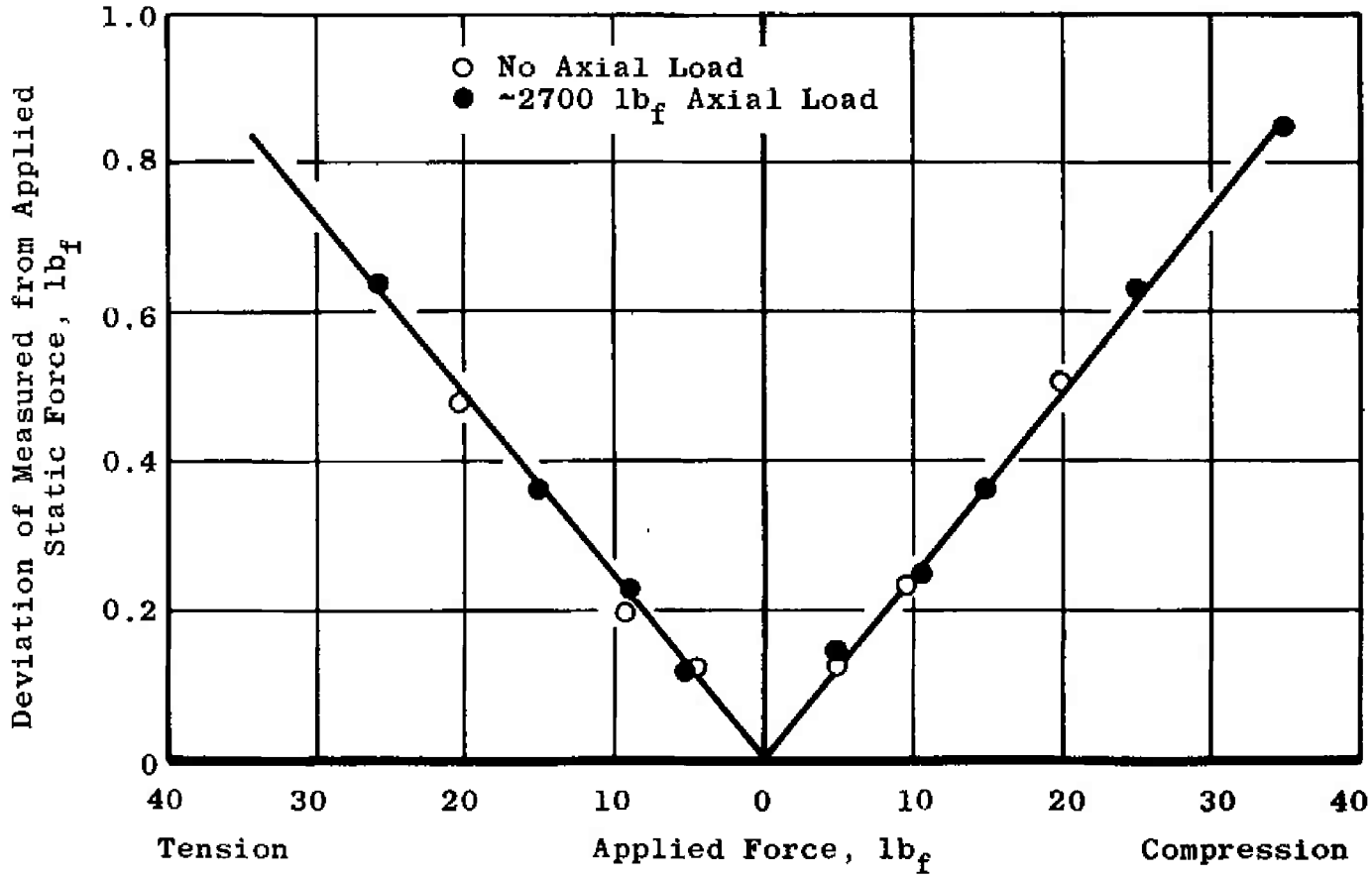

Fig. III-1 Comparison of Measured (Output) and Applied (Input) Forces for Side-Force Static Calibration

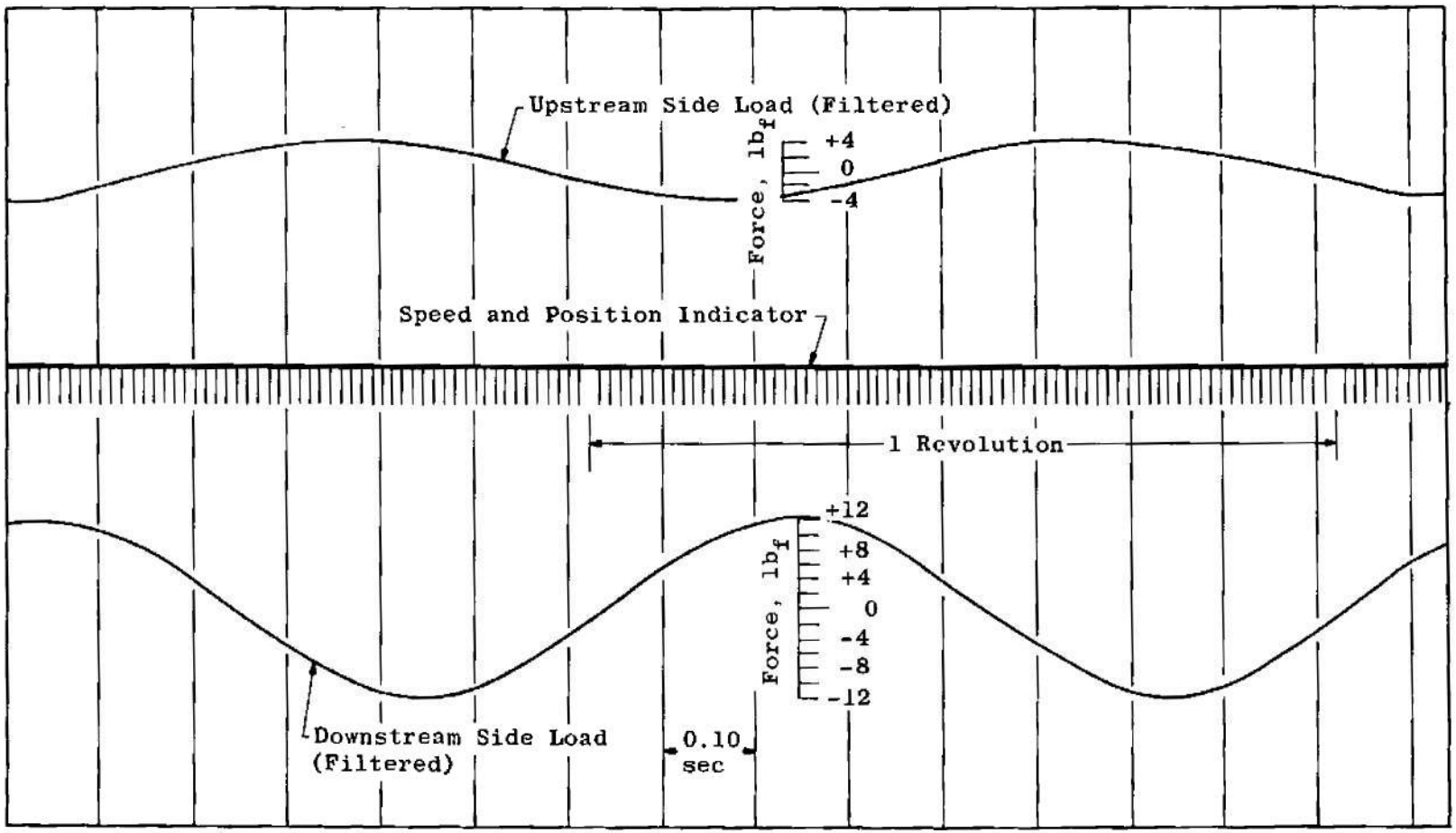

Fig. III-2 Analog Trace of Typical Side-Force Variation of Time

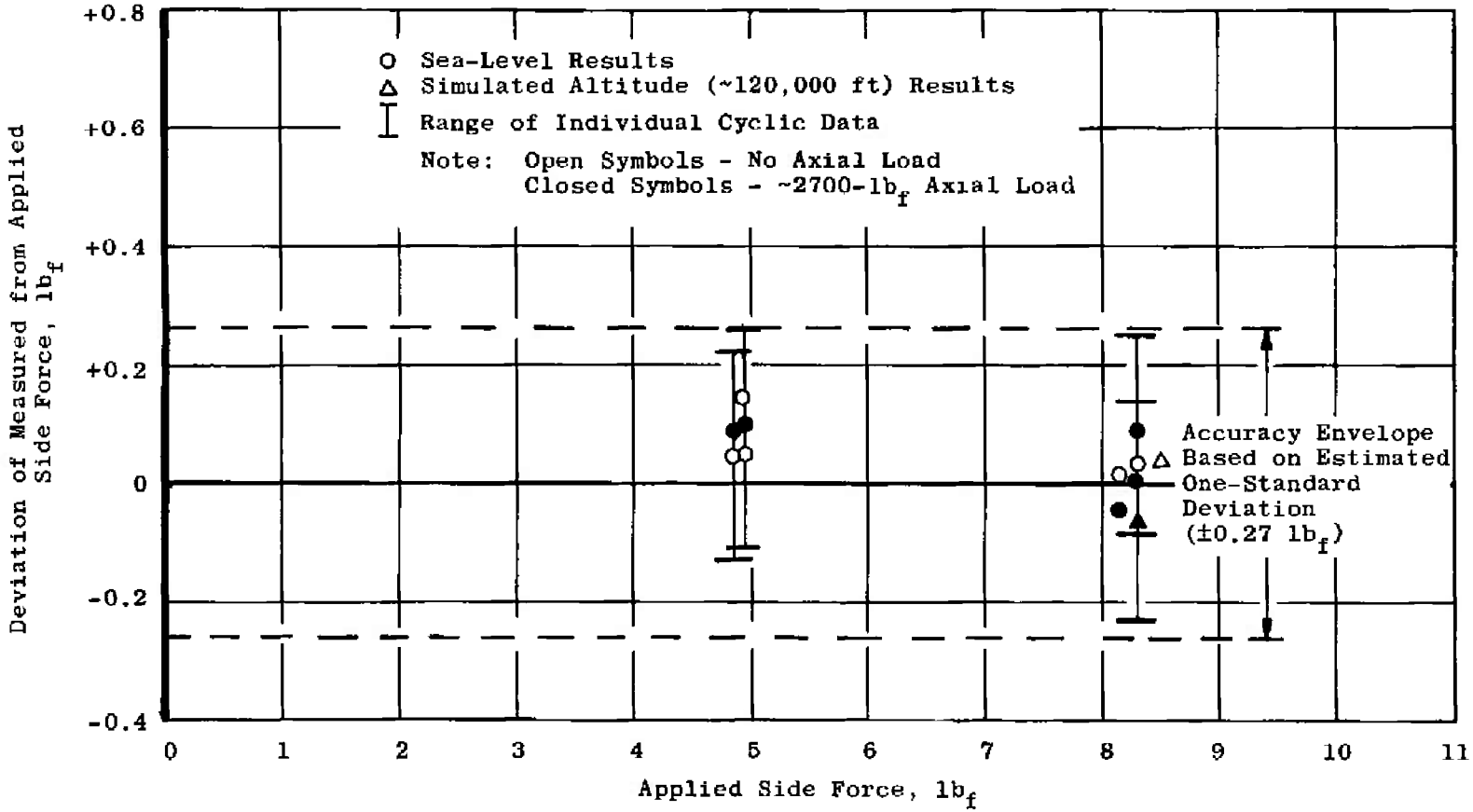

Fig. III-3 Comparison of Measured and Applied Side-Force Values for Spin Calibration to Determine System Accuracy

Security Classification

DOCUMENT CONTROL DATA - R & D

(Security classification of title, body of abstract and indexing annotation must be entered when the overall report is classified)

1 ORIGINATING ACTIVITY (Corporate author)	2a. REPORT SECURITY CLASSIFICATION
Arnold Engineering Development Center ARO, Inc., Operating Contractor Arnold Air Force Station, Tennessee	UNCLASSIFIED
	2b. GROUP N/A

3 REPORT TITLE

EVALUATION OF TWO RADIO ASTRONOMY EXPLORER SPACECRAFT APOGEE KICK MOTORS TESTED IN THE SPIN MODE AT SIMULATED ALTITUDE CONDITIONS

4 DESCRIPTIVE NOTES (Type of report and inclusive dates)

March 24 to 31, 1967 Final Report

5 AUTHOR(S) (First name, middle initial, last name)

D. W. White and J E. Harris, ARO, Inc.

6 REPORT DATE	7a. TOTAL NO. OF PAGES	7b. NO OF REFS
July 1967	63	3

8a. CONTRACT OR GRANT NO	9a. ORIGINATOR'S REPORT NUMBER(S)
AF 40(600)-1200 b. PROJECT NO 9033	AEDC-TR-67-127
c. System 921E	9b. OTHER REPORT NO(S) (Any other numbers that may be assigned this report)
d.	N/A

10 DISTRIBUTION STATEMENT

This document is subject to special export controls and each transmittal to foreign governments or foreign nationals may be made only with prior approval of NASA, Goddard Space Flight Center, Greenbelt, Maryland.

11 SUPPLEMENTARY NOTES	12. SPONSORING MILITARY ACTIVITY
Available in DDC	Goddard Space Flight Center, NASA Greenbelt, Maryland

13 ABSTRACT

Two Thiokol Chemical Corporation TE-M-479 solid-propellant apogee rocket motors each installed in a Radio Astronomy Explorer (RAE) spacecraft shell were fired at average pressure altitudes in excess of 118,000 ft while spinning at 75 rpm. The primary objectives of the test were to: evaluate the ignition characteristics of the motor when ignited with one Pyrogen igniter, determine motor vacuum ballistic performance when pre-conditioned at 40 and 90°F, evaluate motor tailoff characteristics, and evaluate motor structural integrity and determine motor temperature-time history during and after motor operation. Secondary objectives were to measure motor thrust misalignment and thermal inputs into the RAE spacecraft resulting from motor operation. Both motors ignited satisfactorily. Vacuum specific impulse values for the 40 and the 90°F motors were 289.97 and 290.63 lb_f-sec/lb_m, respectively, based on the manufacturer's stated propellant weight.

This document is subject to special export controls and each transmittal to foreign governments or foreign nationals may be made only with prior approval of National Aeronautics and Space Administration, Goodard Space Flight Center, Greenbel., Maryland.

DD FORM 1 NOV 65 1473

Security Classification

14 KEY WORDS	LINK A		LINK B		LINK C	
	ROLE	WT	ROLE	WT	ROLE	WT
Radio Astronomy Explorer Spacecraft						
kick motors						
solid propellants						
ignition characteristics						
ballistic performance						